Mutually opposing activity of PIN7 splicing isoforms is required for auxin-mediated tropic responses in Arabidopsis thaliana

Kashkan, Ivan

2022-01

þÿ K a s h k a n , I , H r t y a n , M , R e t z e r , K , H u m p o l í k o v á , J , J a y a s r e e , A
Vondráková , Z , Simon , S , Rombaut , D , Jacobs , T B , Frilander , M J , Hejátko , J , Friml
þÿ , J , P e t r á a e k , J & R o ~ i k a , K 2 0 2 2 , ' M u t u a l l y o p p o s i n g a c t i v i t y o f
is required for auxin-mediated tropic responses in Arabidopsis thaliana ' , New Phytologist ,
vol. 233 , no. 1 , pp. 329-343 . https://doi.org/10.1111/nph.17792

http://hdl.handle.net/10138/349738
https://doi.org/10.1111/nph.17792

acceptedVersion

MR IVAN KASHKAN (Orcid ID : 0000-0002-1971-8747)
DR SIBU SIMON (Orcid ID : 0000-0002-1998-6741)
PROF. JIRI FRIML (Orcid ID : 0000-0002-8302-7596)
DR JAN PETRÁŠEK (Orcid ID : 0000-0002-6719-2735)

Article type : Original Article

Mutually opposing activity of PIN7 splicing isoforms is required for auxin-mediated tropic responses in *Arabidopsis thaliana*

Ivan Kashkan[1,2], Mónika Hrtyan[2], Katarzyna Retzer[1], Jana Humpolíčková[3], Aswathy Jayasree[2], Roberta Filepová[1], Zuzana Vondráková[1], Sibu Simon[1], Debbie Rombaut[4,5], Thomas B. Jacobs[4,5], Mikko J. Frilander[6], Jan Hejátko[2], Jiří Friml[7], Jan Petrášek[1], Kamil Růžička[1,2]

[1]Laboratory of Hormonal Regulations in Plants, Institute of Experimental Botany, Czech Academy of Sciences, 16502 Prague, Czech Republic; [2]Functional Genomics and Proteomics of Plants, Central European Institute of Technology and National Centre for Biomolecular Research, Masaryk University, 62500 Brno, Czech Republic; [3]Institute of Organic Chemistry and Biochemistry, Czech Academy of Sciences, 166 10 Prague 6, Czech Republic; [4]Department of Plant Biotechnology and Bioinformatics, Ghent University, 9052 Ghent, Belgium; [5]VIB Center for Plant Systems Biology, 9052 Ghent, Belgium; [6]Institute of Biotechnology, University of Helsinki, 00014 University of Helsinki, Finland; [7]Institute of Science and Technology (IST Austria), 3400 Klosterneuburg, Austria

Author for correspondence: Kamil Růžička
Tel: +420 225 106 429
Email: kamil.ruzicka@ueb.cas.cz

Received: *27 June 2021*

Accepted: *3 October 2021*

Authors ORCID information

Ivan Kashkan	https://orcid.org/**0000-0002-1971-8747**
Katarzyna Retzer	https://orcid.org/**0000-0001-6074-7999**
Jana Humpolíčková	https://orcid.org/**0000-0003-4414-2898**
Aswathy Jayasree	https://orcid.org/**0000-0003-2598-8214**
Sibu Simon	https://orcid.org/**0000-0002-1998-6741**
Thomas B. Jacobs	https://orcid.org/**0000-0002-5408-492X**
Mikko J. Frilander	https://orcid.org/**0000-0002-1732-4808**
Jan Hejátko	https://orcid.org/**0000-0002-2622-6046**
Jiří Friml	https://orcid.org/**0000-0002-8302-7596**
Jan Petrášek	https://orcid.org/**0000-0002-6719-2735**
Kamil Růžička	https://orcid.org/**0000-0002-0602-2046**

Summary

- Advanced transcriptome sequencing has uncovered that the majority of eukaryotic genes undergo alternative splicing (AS). Nonetheless, little effort has been dedicated to investigating the functional relevance of particular splicing events, even those in the key developmental and hormonal regulators.
- Combining approaches of genetics, biochemistry and advanced confocal microscopy, we describe the impact of alternative splicing on the *PIN7* gene in the plant model *Arabidopsis thaliana*. *PIN7* encodes a polarly localized transporter for the phytohormone auxin and produces two evolutionary-conserved transcripts *PIN7a* and *PIN7b*.
- PIN7a and PIN7b, differing in a 4-amino acid motif, exhibit almost identical expression pattern and subcellular localization. We reveal that they closely associate and mutually influence their mobility within the plasma membrane. Phenotypic complementation tests indicate that the

functional contribution of PIN7b *per se* is minor, but it markedly reduces the prominent PIN7a activity, which is required for correct seedling apical hook formation and auxin-mediated tropic responses.

- Our results establish alternative splicing of the PIN family as a conserved, functionally relevant mechanism, unveiling an additional regulatory level of auxin-mediated plant development.

Keywords

Auxin, auxin transport, PINs, alternative splicing, plant development, RNA processing, tropic responses, *Arabidopsis thaliana.*

Introduction

Auxin is an essential phytohormone, which plays a role in nearly all aspects of plant development. To flexibly adapt to rapidly-changing environmental cues, directional auxin transport represents a highly dynamic means for triggering downstream morphogenetic processes. PIN-FORMED (PIN) auxin efflux carriers are among the key regulators in this respect. In the past years, many efforts uncovered multiple mechanisms operating transcriptionally or post-translationally on the capacity and directionality of PIN-mediated transport. However, little progress has been made in exploring the contribution of post-transcriptional regulation (Adamowski & Friml, 2015; Hrtyan *et al.*, 2015).

Advances in high throughput sequencing have revealed unexpected complexity within eukaryotic transcriptomes by alternative splicing (AS). Although the majority of AS transcripts may be functionally neutral (Darracq & Adams, 2013; Reddy *et al.*, 2013; Chamala *et al.*, 2015; Tress *et al.*, 2017; Blencowe, 2017), several detailed studies have highlighted a plausible role for numerous AS events in physiologically relevant contexts, including those involved in plant developmental and hormonal pathways (Staiger & Brown, 2013; Hrtyan *et al.*, 2015; Shang *et al.*, 2017; Szakonyi & Duque, 2018). Earlier works have described auxin-related defects resulting from the aberrant function of several regulators of AS (Kalyna *et al.*, 2003; Casson *et al.*, 2009; Retzer *et al.*, 2014; Tsugeki *et al.*, 2015; Hrtyan *et al.*, 2015; Bazin *et al.*, 2018). AS changes subcellular localization of the auxin biosynthetic gene *YUCCA 4* (Kriechbaumer *et al.*, 2012) and differential splicing of an exitron (Marquez *et al.*, 2015) inside the *AUXIN RESPONSE FACTOR 8* (*ARF8*) results in developmental changes of generative organs (Ghelli *et al.*, 2018). Likewise, a splice variant of *MONOPTEROS* (*MP*/*ARF5*) acts as a non-canonical regulator of ovule

development (Cucinotta *et al.*, 2020). In addition, AS of the Major Facilitator Superfamily transporter ZIFL1 interferes with auxin transport, influencing the mobility of PINs in the plasma membrane (PM) (Remy *et al.*, 2013). These lines of evidence indicate that AS is an important player in auxin-dependent processes. However, no coherent functional model of any auxin-related AS event has been provided so far.

Here, we have investigated the functional significance of the protein isoforms arising through AS of the *Arabidopsis thaliana PIN7* gene. PIN7 is, together with PIN3 and PIN4, a member of the PIN3 clade of PIN auxin efflux carriers (Bennett *et al.*, 2014), which are required for a broad range of morphogenetic and tropic processes (Adamowski & Friml, 2015). We provide evidence that the evolutionary conserved PIN7 isoforms mutually influence their dynamics within PM and demonstrate that the coordinated action of both splice variants is required for auxin-mediated differential growth responses.

Materials and Methods

Plant material and plant growth conditions

All plant material, except tobacco cell cultures, was in the *Arabidopsis thaliana* (L.) Heynh., Col-0 ecotype. These mutant and transgenic lines were described previously: *PIN3::PIN3-GFP* (Zadnikova *et al.*, 2010)*, PIN4::PIN4-GFP*, *PIN7::PIN7-GFP* (Blilou *et al.*, 2005), *pin7-2* (Friml *et al.*, 2003), *pin3-3 pin4-101* (*pin34*), *pin3-3 pin4-101 pin7-102* (*pin347*) (Willige *et al.*, 2013). Primers used in the study are listed in Table S1.

For the *in vitro* cultivation, the seeds were surface-sterilized for 5 h with chlorine gas, plated on 0.5× Murashige & Skoog medium with 1 % sucrose and 1 % agar, and then stratified for 2 d at 4°C in darkness. Unless indicated otherwise, the seedlings were grown on vertically oriented plates for 4-6 days under 16 h : 8 h photoperiod, 22 : 18°C, light : dark.

The following chemicals were used for treatments: brefeldin A (BFA), cytochalasin D (CytD), oryzalin (Ory), β-estradiol, 2,4-dichlorophenoxyacetic acid (2,4-D), all from Sigma (Sigma-Aldrich, St. Louis, MO, USA). Radioactively labeled auxin accumulation assays were performed with [^{3}H]NAA (naphthalene-1-acetic acid; 20 Ci.mmol^{-1}; American Radiolabeled Chemicals, St. Louis, MO, USA).

Plant phenotype analysis

The dynamic seedling development was tracked in the custom-made dynamic morphogenesis observation chamber equipped with blue and white LED unilateral light sources, infra-red LED backlight, and a camera for imaging in the infra-red spectra, controlled by the Raspberry Pi3B microcomputer (Raspberry Pi foundation, Cambridge, UK). Image acquisition was controlled by the custom-written python script (https://github.com/lamewarden/RaPiD-boxes-software). For the hypocotyl bending assays, seeds on the plate were first illuminated for 6 h with white light. The plates were then transferred to the observation chamber for 3-4 d. For the hypocotyl phototropic bending experiments (Friml *et al.*, 2002), the dark-grown seedlings were afterward illuminated for 20 h with unilateral white light and imaged every 20 minutes. For hypocotyl gravitropic bending experiments (Rakusová *et al.*, 2011), the dark-grown seedlings were rotated by 90° clockwise and imaged for 30 h every 60 min. For tracking apical hook development, the seeds were first illuminated for 6 h with white light. They were then transferred to the observation chamber and their development was recorded every 4 h for a total 150 - 200 h in infrared spectra. Germination time was set as time 0, when first traces of the main root were observed, individually for each seedling analyzed. Apical hook was determined as an angle between the immobile (non-bending) part of hypocotyl and the distal edge of cotyledons (Zadnikova *et al.*, 2010), using the ImageJ software (Rueden *et al.*, 2017). At least 15 seedlings were analyzed for each line. Each experiment was done at least three times.

For protoxylem defects analysis, 5-d old light-grown seedlings were cleared and analyzed as described previously (Bishopp *et al.*, 2011). For examining lateral root density, 8-d old light-grown seedlings were cleared and observed with a DIC microscope (Dubrovsky *et al.*, 2009). Lateral root density was calculated by dividing the total number of lateral roots and lateral root primordia by the length of the main root as described (Dubrovsky *et al.*, 2009). Vertical Growth Index (VGI), defined as a ratio between main root ordinate and main root length, was quantified on 5-d old seedlings as published previously (Grabov *et al.*, 2005). For measuring the Gravitropic Set-point Angle (GSA), plates with 14-d old light-grown seedlings were scanned, and the angles between the vertical axis and five innermost 0.5 mm parts of lateral root were determined as described previously (Roychoudhry *et al.*, 2017). In all cases, 12-20 seedlings were analyzed for each line. Each experiment was done at least three times.

For decapitation experiments, 4-week short-day grown plants were moved into long-day conditions to induce flowering. After the primary bolt reached 10-15 cm, the plant was decapitated. The number of rosette branches was recorded at 7, 10, and 14-d after decapitation

(Greb *et al.*, 2003; Waldie & Leyser, 2018). Rosette size was inspected in 18-d light-grown plants prior to documenting. 10 plants were analyzed for each line, the experiment was done three times.

Tobacco cell lines and auxin accumulation assays

Tobacco cell line BY-2 (*Nicotiana tabacum* L. cv. Bright Yellow 2) was cultivated as described (Müller *et al.*, 2019). BY-2 cells were transformed with the pMDC7 constructs by co-cultivation with *Agrobacterium tumefaciens* strain GV2260 as earlier described (Petrasek *et al.*, 2006; Müller *et al.*, 2019). The transgene expression was maintained by cultivation on media supplemented with 40 $\mu g.ml^{-1}$ hygromycin (Roche) and 100 $\mu g.ml^{-1}$ cefotaxime (Sigma). Accumulation assays of radioactively labeled auxin were performed as previously published (Delbarre *et al.*, 1996; Petrasek *et al.*, 2006) with cells cultured for 2 days in β-estradiol or DMSO mock treatments. Presented results are from 3 biological replicates for each representative *PIN7a* and *PIN7b* line and were confirmed for each on two other independent genotypes. Independent β-estradiol inductions were done within 3-9 months after establishing the cell suspension on lines, which showed comparable levels of the expressed PIN7-GFP signal.

Microscopy

Bright-field microscopy (differential interference contrast, DIC) was conducted on the Olympus BX61 instrument (Olympus, Shinjuku, Tokyo, Japan) equipped with a DP50 camera (Olympus). Routine confocal microscopy was performed on inverted Zeiss Axio Observer.Z1 containing the standard confocal LSM880 and Airyscan modules with 20x/0.8 DIC M27 air, 40x/1.2 W Kor FCS M27 air and 63x/1.40 Oil DIC M27 objectives (Carl Zeiss AG, Jena, Germany). Gravity-induced polarity change experiments were carried out on Zeiss Axio Observer.Z1 with vertically oriented sample position and the 40x/0.75 glycerol objective.

To observe the light-induced polarity change of PIN7a-GFP and PIN7b-RFP, 4-d dark-grown seedlings were irradiated for 4 h with unilateral white light and then imaged with Zeiss Axio Observer.Z1 LSM880 with a vertically oriented sample position, as described (Willige *et al.*, 2013). For analyzing gravity-induced polarity change, 4-d dark-grown seedlings were reoriented by 90° clockwise and imaged 6 and 24 h after rotation, as described (Rakusová *et al.*, 2011).

For BFA treatments, 5-d light-grown seedlings were transferred to liquid 0.5× MS media containing 50 μM BFA. The membrane/cytosol ratio was determined with ImageJ, it was defined as the mean membrane signal intensity divided by the mean fluorescence in the cytosol. For

cytoskeleton depolymerizing drug treatments (Geldner *et al.*, 2001), 5-d light-grown seedlings were transferred to liquid 0.5× MS media supplemented with 20 μM of cytochalasin D or 20 μM oryzalin. The co-treatments were done by the direct addition of BFA. For the BFA removal, prior to adding the cytoskeleton depolymerizing compounds, seedlings were twice washed out with fresh media and then transferred to that supplemented with the respective cytoskeleton-depolymerizing drug.

For imaging of the expression of *DR5v2:GFP* in the apical hook, the GFP signal in the 4-days old etiolated seedlings was fixed in 4% paraformaldehyde (PFA, Sigma) overnight. Then, the tissue was hand-sectioned with a razor blade and observed.

Fluorescent recovery after photobleaching (FRAP)

For the FRAP experiments, Zeiss Axio Observer.Z1 equipped with the LSM880 confocal and Airyscan modules and the 40x/1.2 W Kor FCS M27 air objective was used. FRAP assay was done and evaluated as described (Sprague & McNally, 2005; Laňková *et al.*, 2016). Normalization and time averaging were done with a python script available via GitHub (https://github.com/lamewarden/FRAP-normalization-script). The Slices Alignment plugin (Tseng *et al.*, 2012) for ImageJ was used to eliminate cell movement caused by root growth.

FLIM-FRET analysis

For assessing the pairing specificity in *Arabidopsis*, the lines harboring all 4 combinations of *G10-90::XVE>>PIN7a/b-GFP* (donors) and *PIN7a/b-RFP* (acceptors) were generated. Before imaging, 4-d light-growth seedlings were transferred for two days to the solid ½ MS media supplemented with 5 μM β-estradiol. The transient expression in tobacco leaves was performed as earlier published (Horák *et al.*, 2008), omitting the β-estradiol induction to keep the transgene expression low (Bashandy *et al.*, 2015). The abaxial epidermis of tobacco leaves was observed 3 days after infiltration.

The procedure of the FRET-FLIM assay was done as previously described (Krejčí *et al.*, 2015). Imaging was performed on inverted Zeiss LSM 780 AxioObserver.Z1 equipped with the M27 Plan-Apochromat 20x air objective, external In-Tune laser (<3 nm width, pulsed, 40 MHz, 1.5 mW) and the GaAsP detectors. For conducting the FLIM-FRET assays, the HPM-100-40 hybrid detector associated with the photon counting module Simple-Tau 150 (compact TCSPC

system based on the SPC-150N device) was utilized, using the detector controller card DCC-100 (Becker & Hickl GmbH, Berlin, Germany).

Statistics and sequence analysis

For the mean comparison of the two groups, Student's *t*-test was applied. Statistical analysis of multiple groups was performed by one-way ANOVA with subsequent Tukey HSD post-hoc test. For the temporal analysis of seedling development, regions with approximately linear courses were selected. Those parallel to the x-axis were evaluated as mean angles of each seedling within the sample by one-way ANOVA. The regions with an apparent slope were fitted with linear regression (Table S2). The regression line intercepts with the y-axis and the slope values were evaluated with one-way ANOVA (Table S3). All statistical tests, including the Shapiro-Wilk test for assessing the normal distribution of variables, were performed in R-studio IDE (R-studio, Boston, MA, USA). In the box plots, the whisker length was set as $Q \pm 1.5 \times \mathrm{IQR}$, where Q is the corresponding quartile, and IQR is the interquartile range. For creating the multiple sequence alignments, the protein sequences were assembled with the Clustal Omega algorithm (Sievers *et al.*, 2011) and graphically outlined by Mega-X, using the default ClustalX color code (Kumar *et al.*, 2018).

Additional methods

DNA manipulation, quantitative RT-PCR, protein extraction, immunoblotting, and co-immunoprecipitation methods and procedures are provided in Methods S1.

Results

***Arabidopsis PIN7* and *PIN4* produce two evolutionary conserved AS transcripts**

Our previous survey (Hrtyan *et al.*, 2015) revealed that several genes involved in auxin-dependent processes undergo AS. Among them, closely related paralogs from the *PIN3* clade of auxin transporters, *PIN4* and *PIN7* (but not *PIN3*), are regulated by the same type of AS (Petrasek *et al.*, 2006; Bennett *et al.*, 2014; Hrtyan *et al.*, 2015). The resulting transcripts, denoted as *a* and *b*, differ in the AS donor site position in the first intron (Fig. 1a). The differentially spliced region corresponds to a four amino acid motif inside the large internal hydrophilic loop (Ganguly *et al.*, 2014; Nodzyński *et al.*, 2016) of the integral PM transporter (Fig. 1a, b). We examined the quantities of individual reads spanning the exon junctions in the respective gene region from the

Arabidopsis root tip and in several other available transcriptomes from different tissues and organs (Klepikova *et al.*, 2016; Cheng *et al.*, 2017; Ruzicka *et al.*, 2017) (Fig. 1c and Table S4). In accord with other data sets (Martín *et al.*, 2021), we found that each of the *PIN4* and *PIN7* splice isoforms is expressed abundantly in all tissues, independently of the inspected data set. We also identified a minor *PIN4c* (Marquez *et al.*, 2012; Hrtyan *et al.*, 2015) transcript (but not corresponding *PIN7c*), which comprised around 3-7% of the *PIN4* exon1-exon2 spanning reads (Fig. 1a and Table S4). Other occasionally observed transcripts (also corresponding to the other exon junctions) were not seen among different RNA-seq data sets. It thereby appears that *PIN7* and *PIN4* are processed into two and three splice isoforms, respectively, and that *PIN7a* and *b* (or *PIN4a* and *b*) are expressed in most plant organs at comparable levels, possibly with a moderate prevalence of *PIN7b* over *PIN7a*.

Functionally relevant AS events are commonly evolutionary conserved (Keren *et al.*, 2010; Reddy *et al.*, 2013). Therefore we sought for available validated transcripts to determine whether similar splicing events occur in orthologous *PIN3* clade genes in other dicot species (Bennett *et al.*, 2014; O'Leary *et al.*, 2016). We found examples of such mRNAs besides members of the *Brassicaceae* family, for instance, in *Hibiscus syriacus* (*Malvaceae*) and *Abrus precatorius* (*Fabaceae*), which document the conservation of this AS event among rosids (Fig. 1d). *PIN4c* did not show any deeper evolutional conservation. Thus, at least some genes of the *PIN3* clade are regulated by the same type of AS across several plant families, which suggests that these AS events may have a biologically relevant function.

PIN7 splice isoforms are functionally distinct

We expressed fluorescently-tagged cDNA versions of the respective *PIN7* and *PIN4* transcripts under their native promoters in *Arabidopsis thaliana*. Their overall expression patterns resembled those of the *PIN7-GFP* and *PIN4-GFP* lines made on the basis of the genomic sequence (Fig. S1a–d). Next, we tested their ability to complement the phenotypes associated with the *PIN7* locus. The phototropic hypocotyl bending is among the classical assays for testing the activity of the PIN3 clade proteins (Friml *et al.*, 2002; Willige *et al.*, 2013). As the *pin7-2* loss of function mutants show a weak phenotype in the laboratory conditions (Friml *et al.*, 2003; Blilou *et al.*, 2005; Willige *et al.*, 2013), we employed a triple *pin3-3 pin4-101 pin7-102* knock out (*pin347*) as a genetic background, which lacks the phototropic response almost completely (Willige *et al.*, 2013). Here, *PIN7a-GFP* cDNA rescued the phototropic bending, while the *PIN7b-RFP* cDNA

did not show any effect, regardless of whether the native (Fig. 1e) or a stronger endodermal *SCR* promoter (Rakusová *et al.*, 2011) (Fig. S1e) was used. The tag choice does not appear to have any effect in these assays, as evidenced by the lines where the fluorophore sequences have been swapped (Fig. 1f). Together, these data indicate that the motif changed by AS alters the function of the PIN7 protein in *Arabidopsis*.

The PIN3 clade auxin efflux carriers have been implicated in many other instances of auxin-mediated development (Adamowski & Friml, 2015). We therefore hypothesized whether the role of the particular isoform could be prevalent in some of them. These processes include: determining of root protoxylem formation (Bishopp *et al.*, 2011) (Fig. 1g), lateral root density (Swarup *et al.*, 2008) (Fig. 1h), vertical direction of the root growth (Friml *et al.*, 2002; Kleine-Vehn *et al.*, 2010; Pernisova *et al.*, 2016) (Fig. S1f), lateral root orthogravitropism (Rosquete *et al.*, 2013) (Fig. S1g), gravity-induced hypocotyl bending (Rakusová *et al.*, 2011) (Fig. S1h), number of rosette branches after decapitation (Bennett *et al.*, 2016) (Fig. S1i) and the overall rosette size (Bennett *et al.*, 2016) (Fig. S1j). In all assays, we found that the *PIN7a-GFP* cDNA usually almost completely rescues the *pin347* phenotypes, while the contribution of *PIN7b-RFP* is smaller or even undetectable.

Fluorescent reporters reveal highly overlapping *PIN7a* and *b* expression

The levels of *PIN7* (and *PIN4*) AS transcripts seem to be at comparable levels in most organs (Fig. 1c and Table S4). However, this may not describe the actual situation at the resolution of individual cells. To address this, we analyzed the P7A$_1$G and P7BR fluorescent reporters (Kashkan *et al.*, 2020), which allow for monitoring the activity of the AS of *PIN7 in planta* and *in situ* (Fig. 2a). Indeed, in most cells, including the primary root tip (Fig. 2b) or the hypocotyl during the light bending assay (Fig. 2c), we observed generally overlapping expression of both isoforms without any apparent tissue preference. Though, there were several instances in the vegetative tissue where the ratio of reporter signals appears to be uneven. These include early lateral root primordia (Fig. 2d), the stomatal lineage ground cells of the cotyledons (Fig. 2e), and the concave side of the opening apical hook (Fig. 2f), where the PIN7b-RFP signal prevailed over that of PIN7a-GFP. Overall, these data corroborate the presence of both isoforms in most cells and suggest that they may function in a coordinated manner.

The combined activity of both PIN7a and PIN7b is required for apical hook formation and tropic responses

The generally overlapping expression of both isoforms and an occasionally exaggerated response of the *pin347* mutants containing the *PIN7a-GFP* transgene (Fig. S1h) prompted us to carefully record the temporal dynamics of the processes linked with the PIN3 clade function. We were even able to capture subtle phenotypes of the single *pin7-2* knock-out allele (Friml *et al.*, 2003) during hypocotyl phototropic bending (Fig. 3a) or apical hook formation (Fig. 3b) (Zadnikova *et al.*, 2010), where we observed accelerated development conferred to the expression of *PIN7a-GFP* again. Thus, the temporal analysis of the complemented *pin7-2* lines underlines that AS of *PIN7* has a role in plant development.

To get detailed insight into the possible shared role of both isoforms, we analyzed apical hook development in the *pin34* mutants (Wilige et al., 2013) along with the *pin347* lines that carried the combinations of both *PIN7* cDNA constructs. The presence of the *PIN7b-RFP* cDNA had generally little effect on the severe *pin347* phenotype. Expression of the *PIN7a-GFP* cDNA in *pin347* indeed led to partial rescue of the phenotypic defects, surpassing the values observed for *pin34*. Interestingly, the simultaneous expression of both *PIN7a-GFP* and *PIN7b-RFP* suppressed the dominant effects conferred by the *PIN7a-GFP* cDNA alone and phenocopied the *pin34* mutant (Fig. 3c). It therefore appears that both *PIN7* isoforms act in a coordinated manner.

Relatively complicated apical hook development involves several bending steps (Zadnikova *et al.*, 2010), and the splicing reporter shows differences in epidermal expression of *PIN7a* and *b* on its inner side (Fig. 2f). The hypocotyl photo- and gravitropic response requires only a single bending (Rakusová *et al.*, 2011, 2016), and the reporter fluorescence ratio remains unchanged during stimulation (Fig. 2c). It can thus provide a hint to whether one can account for the antagonistic behavior of both isoforms to differential expression or to another mechanism, probably occurring at the cellular level. Similar to apical hook development, the presence of the *PIN7b-RFP* cDNA had a marginal effect on the *pin347* phenotype during the whole time range recorded, while the expression of *PIN7a-GFP* lead to faster bending than that observed for the *pin34* mutant. Finally, the presence of both *PIN7a-GFP* and *PIN7b-RFP* cDNAs in *pin347* was reminiscent of the *pin34* phenotype in both phototropic and gravity assays (Figs 3d and S2a). The transcript levels attributed to PIN7a-GFP cDNA did not exceed the internal levels of the *PIN7* transcript in the *pin34* mutant, nor did the co-expression of PIN7b-RFP reduce the PIN7a-GFP levels in the *pin347* seedlings (Figs 3c and S2b–d). We therefore conclude that the joint activity of

both PIN7 isoforms located in the same group of cells is required for correct auxin-mediated tropic responses, and these developmental changes cannot be ascribed to the altered balance of the *PIN7* transcripts during tropic assays.

PIN7a, but not PIN7b, can form auxin maxima *in planta*

To further investigate the impact of AS on the PIN7 protein function, we validated the formation of the downstream auxin response maxima in apical hooks by crossing the *DR5v2:GFP* transcriptional auxin reporter (Liao *et al.*, 2015) into lines where the phenotypic changes have been temporally monitored (see Fig. 3). The reporter expression pattern in the forming apical hooks of *pin34*, *PIN7a-GFP pin347* and *PIN7a-GFP PIN7b-RFP pin347* resembled the situation in the wild type (Zadnikova *et al.*, 2016), whereas the *DR5v2:GFP* distribution in the *PIN7b-RFP pin347* line was indistinguishable from that of *pin347* (Fig. 4a). These results underline that the PIN7b isoform alone is unable to establish the morphogenic auxin gradients and that the observed developmental changes occur in line with previously described mechanisms (Friml *et al.*, 2002; Zadnikova *et al.*, 2010, 2016; Willige *et al.*, 2013).

PIN7a and PIN7b transport auxin with comparable rates in tobacco cells

Because PIN7a and PIN7b showed differential ability to generate auxin maxima *in planta*, we asked whether both protein isoforms indeed function as auxin transporters. We expressed the *PIN7a* and *b* cDNA variants tagged with GFP under the control of the β-estradiol-driven promoter in the tobacco BY-2 tissue culture system (Petrasek *et al.*, 2006; Müller *et al.*, 2019). We confirmed that PIN7a (Petrasek *et al.*, 2006), as well as the PIN7b isoform, are functional auxin transporters. To this end, we also analyzed the quantitative aspects of PIN7-mediated transport, using multiple concentrations of β-estradiol. Following induction of both transgenes, we observed a comparable decrease of radioactive-labeled auxin accumulation inside the BY-2 cells for both lines in the β-estradiol dose range used (Fig. 4b), consistent with the similar PIN7a and PIN7b protein levels (Fig. S3a–3c). The time course of the auxin accumulation drop appeared to be similar for both constructs (Fig. 4b). Hence, *PIN7a* and *PIN7b* code for true auxin exporters, and they seem to transport auxin in tobacco cell cultures at similar rates.

PIN7a and PIN7b differ in protein subcellular dynamics

Polarity and dynamic intracellular trafficking are essential functional attributes of PINs (Adamowski & Friml, 2015). However, the PIN7 isoforms did not prominently differ from each other in terms of polarity or general subcellular localization in the root tip at a given resolution limit (Fig. 4c). The anterograde trafficking of proteins towards PM can be effectively blocked by the fungal toxin brefeldin A (BFA). It leads to internal accumulation of the membrane-bound PINs into characteristic BFA bodies (Geldner *et al.*, 2001; Kleine-Vehn *et al.*, 2010). During time-lapse imaging, we observed that while PIN7a-GFP accumulated readily in these intracellular aggregates. The PIN7b-RFP BFA bodies were less pronounced and co-localized with PIN7a-GFP incompletely (Fig. 4c). To exclude the effects of diverse fluorescent tags, we compared the response of PIN7a-GFP to the PIN7b-GFP cDNA lines. The BFA-mediated aggregation of PIN7b-GFP indeed showed a moderate delay compared with PIN7a-GFP (Fig. 4d). It suggests that the PIN7 isoforms differ in the speed of their intracellular trafficking pathways or delivery to the PM, and the choice of the tag does not appear to interfere significantly with the subcellular dynamics of PIN7.

PIN polarity does not seem to strictly require the cytoskeleton (Glanc *et al.*, 2019), but subcellular PIN trafficking has been proposed to be mediated by two distinct pathways (Geldner *et al.*, 2001; Glanc *et al.*, 2019). The first depends on actin filaments (cytochalasin D-sensitive) and occurs in most root meristem cells. The second (oryzalin-sensitive) utilizes microtubules and is linked with cytokinesis. Drugs that depolymerize actin filaments (cytochalasin D) and tubulin (oryzalin) (Geldner *et al.*, 2001; Kleine-Vehn *et al.*, 2008) showed only little effect on the intracellular localization of both PIN7 isoforms when applied alone (Fig. S3d, e). Pretreatment with cytochalasin D prevented the formation of the BFA bodies (Geldner *et al.*, 2001) containing both PIN7 isoforms (Fig. S3f). Yet, when we applied oryzalin prior to the BFA treatment, the BFA compartments with PIN7a-GFP and PIN7b-RFP associated in only very weakly co-localizing structures (Fig. S3g). Next, we tested how the cytoskeleton is involved in the trafficking of both PIN7 isoforms from the BFA bodies to the PM by washing out BFA with cytochalasin D or oryzalin (Geldner *et al.*, 2001). In the presence of cytochalasin D, PIN7a-GFP largely persisted inside the BFA bodies, while the PIN7b-RFP signal was almost absent in these aggregates (Fig. S3h). We generally did not see any difference between both isoforms when BFA was washed out with oryzalin (Fig. S3i). These data thereby suggest that both PIN7 isoforms use vesicle trafficking pathways assisted by a common cytoskeletal scaffold. These pathways differ in their dynamics and the endomembrane components involved and are consistent with previous findings

that individual PINs can utilize multiple PM delivery routes (Boutté *et al.*, 2006; Kleine-Vehn *et al.*, 2008).

PIN7a and PIN7b do not differ in tropic stimuli-mediated polarity change or dimer formation

Auxin transporters of the PIN3 clade change their polar localization on the PM by reacting to various environmental cues, particularly by switching the light or gravity vectors (Friml *et al.*, 2002; Rakusová *et al.*, 2011; Ding *et al.*, 2011). PIN3 relocation in response to gravity in columella root cells is seen in as little as 2 min, while the relocation of PIN7-GFP requires approximately 30 min to be detected (Friml *et al.*, 2002; Kleine-Vehn *et al.*, 2010; Pernisova *et al.*, 2016; Grones *et al.*, 2018). We examined plants harboring both *PIN7a-GFP* and *PIN7b-RFP* cDNAs under short and long gravitropic stimuli. We did not find any difference in relocation dynamics between both isoforms in these experiments (Fig. S4a–b). We also observed no difference in the polarity change between PIN7a-GFP and PIN7b-RFP in hypocotyl gravitropic (Rakusová *et al.*, 2011, 2016) and phototropic (Ding *et al.*, 2011) bending assays (Fig. S4c); due to limited transparency of hypocotyls, we used lines expressing the cDNAs under control of a stronger *SCR* promoter (Rakusová *et al.*, 2011). The different subcellular pathways driving both PIN7a-GFP and PIN7b-RFP cargos are thereby not connected with their ability to change polarity in response to tropic stimuli.

AS frequently changes the protein function by altering their ability to multimerize (Kelemen *et al.*, 2013), and PIN proteins have recently been found to associate in higher-order complexes in tissue cell cultures (Teale *et al.*, 2020; Abas *et al.*, 2021). To independently corroborate these findings, we used the extracts from both *Arabidopsis* seedlings and BY-2 cells, expressing the respective cDNAs, followed by native protein gel electrophoresis and western blotting (Leitner *et al.*, 2012). Probing with anti-GFP antibody indeed revealed a faint protein band at the predicted size of tagged PIN7 dimers in both tissue sources (Fig. S4d–g). Next, using anti-RFP-specific antibody coupled with agarose beads (Waidmann *et al.*, 2018), we performed the co-immunoprecipitation of crude extracts from the *Arabidopsis* seedlings inducibly expressing both *PIN7a-GFP* and *PIN7b-RFP* cDNAs. Examining the precipitates by western blotting further indicated that isoforms can interact (Fig. 4e, f). We further validated these findings with Förster resonance energy transfer by fluorescence lifetime imaging (FRET-FLIM), analyzing the cDNAs expressed stably in *Arabidopsis* seedlings and transiently in the tobacco leaves (Figs 4g, 4h and S4h, S4i). Here, we

also tested the combinations of the GFP and RFP-tagged *PIN7a* and *PIN7b* cDNAs to determine their pairing preference. Shortening of the GFP fluorescence lifetime was seen regardless of the isoform interaction examined and also when expressed under *SCR* promoter (Fig. S4j). However, no changes were observed when another protein located on PM, aquaporin PIP2-GFP (expressed under strong promoter), was used (Fig. S4k). These data therefore suggest that the PIN7 splice isoforms can mutually associate into dimers (or other higher-order complexes), but it seems the strength of their mutual interaction remains comparable.

PIN7a and PIN7b show distinct mobility within PM

Numerous studies employed fluorescence recovery after photobleaching (FRAP) to investigate the dynamic turnover of various proteins, including PINs, on PM. Some suggest that decreased lateral mobility may impact PIN-mediated auxin transport (Men *et al.*, 2008; Martinière *et al.*, 2012; Laňková *et al.*, 2016; Glanc *et al.*, 2021). We therefore bleached a region of the PM signal in the root meristem of the *PIN7a-GFP* and *PIN7b-GFP* cDNA lines and measured the FRAP in this area. Notably, PIN7a-GFP showed a slower recovery of fluorescence than PIN7b-GFP (Fig. 5a); the use of either GFP or RFP tag did not markedly influence the fluorescence recovery (Fig. S5a). We also generated plants carrying a *PIN3::PIN3Δ-RFP* cDNA construct, which lacks the GETK motif corresponding to the four amino acids absent in PIN7b (Figs 1b and 5b). The PIN3Δ-RFP signal displayed an incomplete co-localization with the wild type PIN3-GFP variant in the BFA bodies (Fig. S5b) and faster recovery on the PM, similar to that observed for PIN7a and PIN7b (Fig. 5a, b). It therefore appears that the motif altered by AS of PIN7 is required for the regulation of dynamics of individual isoforms within the PM.

The fluorophore-tagged *PIN7* cDNAs showed a relatively weak signal under natural promoter and biasing the obtained data by extensive bleaching by prolonged confocal imaging (Fig. 5a). Therefore, we utilized the *SCR* promoter-driven lines, which displayed higher expression levels, but still lower intensities than the commonly used genomic DNA-derived *PIN7:PIN7-GFP* (Blilou *et al.*, 2005) (Fig. S5c, d). Indeed, these lines allowed for detecting a finer difference in FRAP compared to those under the control of the native promoter (Fig. 5c). The FRAP experiments (Fig. 5a) were conducted initially on the *pin347* lines, which expressed the corresponding transgenes separately. Therefore, we compared the FRAP values of the single PIN7a-GFP and PIN7b-RFP with those carrying these constructs simultaneously in the *pin347* genetic background. Strikingly, the co-expression of PIN7a-GFP decreased the FRAP of PIN7b-

RFP and, *vice versa*, the presence of PIN7b-RFP increased the FRAP of PIN7a-GFP (Fig. 5c). This shows that the PIN7 isoforms mutually influence their mobility within PM, presumably by the association in a molecular complex.

In addition, both PIN7a and PIN7b did not markedly differ in their capability to transport auxin in the BY-2 cells (Figs 4b and S3a–c). We were unable to detect homologous AS events in plant lineages related to tobacco (see Fig. 1d). We tested FRAP of the *Arabidopsis* PIN7a- and PIN7b-GFP on PM in BY-2 cells. Interestingly, the recovery of both isoforms showed a virtually identical course (Fig. 5d). Altogether, the observations here and above support the scheme that both isoforms physically interact and mutually influence each other mobility within PM, which leads to a differential impact on the plant phenotype.

Discussion

In this work, we present functional evidence that AS increases the diversity among the PIN auxin transporters in *Arabidopsis thaliana* and introduce AS as a valid regulator of auxin transport. Concentrating on PIN7, we reveal that both PIN7a and PIN7b isoforms (differing by the presence of a 4-amino acid stretch) are required together for proper apical hook formation and hypocotyl tropic responses. Genetically evidenced cooperative modes of action of splice isoforms have been earlier proposed during *Arabidopsis* development (Szakonyi & Duque, 2018). The seed dormancy regulator *DELAY OF GERMINATION 1* (*DOG1*) is processed into five mRNAs. Only the expression of two or more DOG1 cDNAs under the native promoter rescues the *dog1* phenotype by synergistic stabilization of the protein by its multimerization (Nakabayashi *et al.*, 2015). The transcriptional factor HYH (HY5 HOMOLOG) possesses an isoform, which lacks a domain required for proteasomal degradation, which leads to its increased stability and probably works as a semi-dominant splice variant (Sibout *et al.*, 2006; Szakonyi & Duque, 2018); this can probably also be the case of the AS of *MONOPTEROS* (Cucinotta *et al.*, 2020). Together with, e. g., a partly similar mechanism described for the temperature-mediated regulation of flowering (Lee *et al.*, 2013; Posé *et al.*, 2013), the example of AS of PIN7 is among rarely described instances where the mutually antagonistic effects of two splice isoforms are observed in the developmental context.

The *PIN7a/b* (*PIN4a/b*) AS event is conserved among rosids, a plant phylogenetic group that radiated more than 100 million years ago (Li *et al.*, 2019). It appears that it has been present in the ancestral rosid *PIN3*-clade and, in *Arabidopsis*, it has remained in the *PIN7* and *PIN4* genes.

The phenotypes of the individual *PIN3*-clade genes are weak but detectable under standard laboratory growth conditions (Simaskova et al., 2015; Rosquete et al., 2018; Robert et al., 2013; Ogura et al., 2019; Fig. 3a, b), and it seems that the subtle defects resulting from the disruption of the single *PIN3*-clade genes can be more pronounced under specific environmental cues (Adamowski & Friml, 2015; Ogura *et al.*, 2019), where joint AS of *PIN7* and *PIN4* may play a role. Although publicly available transcriptomic resources do not indicate that the expression of the individual *PIN7* or *PIN4* isoforms is dramatically changed under a wide range of experimental conditions (Martín *et al.*, 2021), we observed that the *PIN7a* expression could be lowered by the application of exogenous auxin (Kashkan *et al.*, 2020). Considering that disabling several factors involved in AS leads to auxin-related defects (Kalyna *et al.*, 2003; Casson *et al.*, 2009; Retzer *et al.*, 2014; Tsugeki *et al.*, 2015; Hrtyan *et al.*, 2015; Bazin *et al.*, 2018), this mode of regulation of AS of *PIN7* (and *PIN4*) proposes the existence of an unknown auxin-mediated pathway, active at the post-transcriptional level.

AS modifies protein properties variably. It affects subcellular localization, ligand binding affinity, enzymatic or transporting activities, protein stability, or the presence of covalent post-translational modifications (Stamm *et al.*, 2005; Kelemen *et al.*, 2013). Different covalent modifications alter the subcellular trafficking of most PINs. Phosphorylation sites on serine, threonine, or tyrosine residues of various PINs have been identified; their phosphorylation status also changes PIN-mediated tropic responses (Rademacher & Offringa, 2012; Barbosa *et al.*, 2018; Zwiewka *et al.*, 2019). Also PIN ubiquitination (on lysines) and controlled proteolytic degradation act in auxin-mediated processes (Leitner *et al.*, 2012). However, none of the candidate residues required for these modifications is present in the vicinity of the amino acid motif changed by AS. This region in the PIN long hydrophilic loop is, inferring from the low amino acid conservation (Fig. 1b), probably intrinsically disordered. Therefore, one can speculate whether just the length of this motif can be critical for functional interaction among internal structural domains (Buljan *et al.*, 2013). These structural differences may modulate the affinity of PINs to bind the factors required for the entry and presence in the membrane secretory pathways, and thus participate in the PIN subcellular dynamics and directional auxin transport.

In this work, we validated the most plausible hypotheses (Adamowski & Friml, 2015) to provide a mechanistic view on the observed mutual functionality of PIN7a and PIN7b. This AS event neither affects the capability of PIN7 carriers to transport auxin *per se* nor influences their ability to relocate after the tropic stimulus. Although we occasionally noticed some expression

irregularities, it seems that the expression changes are unlikely to explain the distinct contributions of PIN7 isoforms to plant development. Instead, our data favor the scenario that PIN7a and PIN7b functionally interact at the protein level. Moreover, we demonstrate with orthogonal experimental approaches that PIN7 isoforms closely associate (Teale *et al.*, 2020; Abas *et al.*, 2021) in native plant tissues and influence each other's mobility within PM. It has previously been suggested that PINs are complexed inside stable integral PM clusters (Feraru *et al.*, 2011; Li *et al.*, 2021). Although the proposed molecular model can be more complicated (Zourelidou *et al.*, 2014; Weller *et al.*, 2017), the mobility of PINs within PM (described as lateral diffusion) has been recently linked with the activity of the AGC kinases and MAB4/MEL proteins (Glanc *et al.*, 2021), whose loss-of-function mutations phenocopy *pin* mutants (Bennett *et al.*, 1995; Furutani *et al.*, 2007). We reveal that mobility on PM is indeed required for the PIN-mediated auxin transport. In this scheme, PIN7a, detained inside the PM microdomains, transports auxin, but dynamic PIN7b does not. Hence, PIN7b binds PIN7a, reducing its presence in these membrane domains and thereby impedes the polar auxin flow to mediate auxin developmental responses (Fig. S5e).

Acknowledgements

We thank Claus Schwechheimer for the *pin34* and *pin347* seeds, Yuliia Mironova for technical assistance, Ksenia Timofeyenko and Dmitry Konovalov for help with the evolutional analysis, Konstantin Kutashev and Siarhei Dabravolski for the assistance with FRET-FLIM, Huibin Han for advice with the hypocotyl imaging, Karel Müller for the initial qRT-PCR on the tobacco cell lines, Stano Pekár for suggestions to the statistical analysis of the morphodynamic measurements, and Jozef Mravec, Dolf Weijers and Lindy Abas for their comments on the manuscript. This work was supported by the Czech Science Foundation (projects 16-26428S and 19-23773S to I. K., M. H. and K. Rů, 19-18917S to J. Hu. and 18-26981S to J. F.), and the Ministry of Education, Youth and Sports of the Czech Republic (MEYS, CZ.02.1.01/0.0/0.0/16_019/0000738) to K. Rů. and J.H.. The imaging facilities of the Institute of Experimental Botany and CEITEC are supported by MEYS (LM2018129 - Czech BioImaging and CZ.02.1.01/0.0/0.0/16_013/0001775). The authors declare no competing interests.

Author contributions

I. K., M. H., K. Re., J. Hu., A. J., R. F., Z. V., D. R., and J. P. conducted experiments. S. S. and J. F. provided unpublished material. I. K., M. J. F., J. P., and K. Rů. conceptualized the research. I. K., K. Re., J. Hu., J. P., T. B. J., J. He., J. F., J. P., and K. Rů. and designed experiments. K. Rů. and I. K. wrote the manuscript. All authors read and approved the final version of the manuscript.

Data Availability Statement

The data that support the findings of this study and all generated material, such as cloned plasmids, BY-2 cell cultures, and *Arabidopsis* seeds used in the study, will be made available from the corresponding author (K.Rů.) upon request. Sequences of the primers used in the study are provided in the Table S1. All protocols and methods used in the study are described in the Materials and Methods and Methods S1 sections. All programming code used in the study is available online on GitHub.com (https://github.com/lamewarden/RaPiD-boxes-software and https://github.com/lamewarden/FRAP-normalization-script).

References

Abas L, Kolb M, Stadlmann J, Janacek DP, Lukic K, Schwechheimer C, Sazanov LA, Mach L, Friml J, Hammes UZ. **2021**. Naphthylphthalamic acid associates with and inhibits PIN auxin transporters. *Proceedings of the National Academy of Sciences* **118**: e2020857118.

Adamowski M, Friml J. **2015**. PIN-dependent auxin transport: action, regulation, and evolution. *The Plant Cell* **27**: 20–32.

Barbosa ICR, Hammes UZ, Schwechheimer C. **2018**. Activation and polarity control of PIN-FORMED auxin transporters by phosphorylation. *Trends in Plant Science* **23**: 523–538.

Bashandy H, Jalkanen S, Teeri TH. **2015**. Within leaf variation is the largest source of variation in agroinfiltration of *Nicotiana benthamiana*. *Plant Methods* **11**: 47.

Bazin J, Romero N, Rigo R, Charon C, Blein T, Ariel F, Crespi M. **2018**. Nuclear Speckle RNA binding proteins remodel alternative splicing and the non-coding *Arabidopsis* transcriptome to regulate a cross-talk between auxin and immune responses. *Frontiers in Plant Science* **9**: 1209.

Bennett SRM, Alvarez J, Bossinger G, Smyth DR. **1995**. Morphogenesis in *pinoid* mutants of *Arabidopsis thaliana*. *The Plant Journal* **8**: 505–520.

Bennett T, Brockington SF, Rothfels C, Graham SW, Stevenson D, Kutchan T, Rolf M, Thomas P, Wong GK-S, Leyser O, *et al.* 2014. Paralogous radiations of PIN proteins with multiple origins of noncanonical PIN structure. *Molecular Biology and Evolution* **31**: 2042–2060.

Bennett T, Hines G, Rongen M van, Waldie T, Sawchuk MG, Scarpella E, Ljung K, Leyser O. **2016**. Connective auxin transport in the shoot facilitates communication between shoot apices. *PLoS Biology* **14**: e1002446.

Bishopp A, Help H, El-Showk S, Weijers D, Scheres B, Friml J, Benková E, Mähönen AP, Helariutta Y. **2011**. A mutually inhibitory interaction between auxin and cytokinin specifies vascular pattern in roots. *Current Biology* **21**: 917–926.

Blencowe BJ. **2017**. The relationship between alternative splicing and proteomic complexity. *Trends in Biochemical Sciences* **42**: 407–408.

Blilou I, Xu J, Wildwater M, Willemsen V, Paponov I, Friml J, Heidstra R, Aida M, Palme K, Scheres B. **2005**. The PIN auxin efflux facilitator network controls growth and patterning in *Arabidopsis* roots. *Nature* **433**: 39–44.

Boutté Y, Crosnier M-T, Carraro N, Traas J, Satiat-Jeunemaitre B. **2006**. The plasma membrane recycling pathway and cell polarity in plants: studies on PIN proteins. *Journal of Cell Science* **119**: 1255–1265.

Buljan M, Chalancon G, Dunker AK, Bateman A, Balaji S, Fuxreiter M, Babu MM. **2013**. Alternative splicing of intrinsically disordered regions and rewiring of protein interactions. *Current Opinion in Structural Biology* **23**: 443–450.

Casson SA, Topping JF, Lindsey K. **2009**. MERISTEM-DEFECTIVE, an RS domain protein, is required for the correct meristem patterning and function in *Arabidopsis*. *The Plant Journal* **57**: 857–869.

Chamala S, Feng G, Chavarro C, Barbazuk WB. **2015**. Genome-wide identification of evolutionarily conserved alternative splicing events in flowering plants. *Frontiers in Bioengineering and Biotechnology* **3**: 33.

Cheng C-Y, Krishnakumar V, Chan AP, Thibaud-Nissen F, Schobel S, Town CD. **2017**. Araport11: a complete reannotation of the *Arabidopsis thaliana* reference genome. *The Plant Journal* **89**: 789–804.

Cucinotta M, Cavalleri A, Guazzotti A, Astori C, Manrique S, Bombarely A, Oliveto S, Biffo S, Weijers D, Kater MM, *et al.* 2020. Alternative splicing generates a MONOPTEROS isoform required for ovule development. *Current Biology* **31**: 892–899.

Darracq A, Adams KL. **2013**. Features of evolutionarily conserved alternative splicing events between *Brassica* and *Arabidopsis*. *New Phytologist* **199**: 252–263.

Delbarre A, Muller P, Imhoff V, Guern J. **1996**. Comparison of mechanisms controlling uptake and accumulation of 2,4-dichlorophenoxy acetic acid, naphthalene-1-acetic acid, and indole-3-acetic acid in suspension-cultured tobacco cells. *Planta* **198**: 532–541.

Ding Z, Galván-Ampudia CS, Demarsy E, Łangowski Ł, Kleine-Vehn J, Fan Y, Morita MT, Tasaka M, Fankhauser C, Offringa R, *et al.* 2011. Light-mediated polarization of the PIN3 auxin transporter for the phototropic response in *Arabidopsis*. *Nature Cell Biology* **13**: 447–452.

Dubrovsky JG, Soukup A, Napsucialy-Mendivil S, Jeknic Z, Ivanchenko MG. **2009**. The lateral root initiation index: an integrative measure of primordium formation. *Annals of Botany* **103**: 807–817.

Feraru E, Feraru MI, Kleine-Vehn J, Martinière A, Mouille G, Vanneste S, Vernhettes S, Runions J, Friml J. **2011**. PIN Polarity Maintenance by the cell wall in *Arabidopsis*. *Current Biology* **21**: 338–343.

Friml J, Vieten A, Sauer M, Weijers D, Schwarz H, Hamann T, Offringa R, Jürgens G. **2003**. Efflux-dependent auxin gradients establish the apical-basal axis of *Arabidopsis*. *Nature* **426**: 147–153.

Friml J, Wiśniewska J, Benková E, Mendgen K, Palme K. **2002**. Lateral relocation of auxin efflux regulator PIN3 mediates tropism in *Arabidopsis*. *Nature* **415**: 806–809.

Furutani M, Kajiwara T, Kato T, Treml BS, Stockum C, Torres-Ruiz RA, Tasaka M. **2007**. The gene *MACCHI-BOU 4*/*ENHANCER OF PINOID* encodes a NPH3-like protein and reveals similarities between organogenesis and phototropism at the molecular level. *Development* **134**: 3849–3859.

Ganguly A, Park M, Kesawat MS, Cho H-T. **2014**. Functional Analysis of the hydrophilic loop in intracellular trafficking of *Arabidopsis* PIN-FORMED proteins. *The Plant Cell* **26**: 1570–1585.

Geldner N, Friml J, Stierhof YD, Jürgens G, Palme K. **2001**. Auxin transport inhibitors block PIN1 cycling and vesicle trafficking. *Nature* **413**: 425–428.

Ghelli R, Brunetti P, Napoli N, Paolis AD, Cecchetti V, Tsuge T, Serino G, Matsui M, Mele G, Rinaldi G, *et al.* 2018. A newly identified flower-specific splice variant of AUXIN RESPONSE FACTOR 8 regulates stamen elongation and endothecium lignification in *Arabidopsis*. *The Plant Cell* **30**: 620–637.

Glanc M, Fendrych M, Friml J. **2019**. PIN2 polarity establishment in *Arabidopsis* in the absence of an intact cytoskeleton. *Biomolecules* **9**: 222.

Glanc M, Gelderen KV, Hoermayer L, Tan S, Naramoto S, Zhang X, Domjan D, Včelařová L, Hauschild R, Johnson A, *et al.* 2021. AGC kinases and MAB4/MEL proteins maintain PIN polarity by limiting lateral diffusion in plant cells. *Current Biology* **31**: 1918–1930.

Grabov A, Ashley MK, Rigas S, Hatzopoulos P, Dolan L, Vicente-Agullo F. **2005**. Morphometric analysis of root shape. *The New Phytologist* **165**: 641–651.

Greb T, Clarenz O, Schafer E, Muller D, Herrero R, Schmitz G, Theres K. **2003**. Molecular analysis of the *LATERAL SUPPRESSOR* gene in *Arabidopsis* reveals a conserved control mechanism for axillary meristem formation. *Genes & Development* **17**: 1175–1187.

Grones P, Abas M, Hajný J, Jones A, Waidmann S, Kleine-Vehn J, Friml J. **2018**. PID/WAG-mediated phosphorylation of the *Arabidopsis* PIN3 auxin transporter mediates polarity switches during gravitropism. *Scientific Reports* **8**: 10279.

Horák J, Grefen C, Berendzen KW, Hahn A, Stierhof Y-D, Stadelhofer B, Stahl M, Koncz C, Harter K. **2008**. The *Arabidopsis thaliana* response regulator ARR22 is a putative AHP phospho-histidine phosphatase expressed in the chalaza of developing seeds. *BMC Plant Biology* **8**: 77.

Hrtyan M, Šliková E, Hejátko J, Růžička K. **2015**. RNA processing in auxin and cytokinin pathways. *Journal of Experimental Botany* **66**: 4897–4912.

Kalyna M, Lopato S, Barta A. **2003**. Ectopic expression of *atRSZ33* reveals its function in splicing and causes pleiotropic changes in development. *Molecular Biology of the Cell* **14**: 3565–3577.

Kashkan I, Timofeyenko K, Kollárová E, Růžička K. **2020**. In vivo reporters for visualizing alternative splicing of hormonal genes. *Plants* **9**: 868.

Kelemen O, Convertini P, Zhang Z, Wen Y, Shen M, Falaleeva M, Stamm S. **2013**. Function of alternative splicing. *Gene* **514**: 1–30.

Keren H, Lev-Maor G, Ast G. **2010**. Alternative splicing and evolution: diversification, exon definition and function. *Nature Reviews Genetics* **11**: 345–355.

Kleine-Vehn J, Ding Z, Jones AR, Tasaka M, Morita MT, Friml J. **2010**. Gravity-induced PIN transcytosis for polarization of auxin fluxes in gravity-sensing root cells. *Proceedings of the National Academy of Sciences* **107**: 22344–22349.

Kleine-Vehn J, Łangowski Ł, Wiśniewska J, Dhonukshe P, Brewer PB, Friml J. **2008**. Cellular and molecular requirements for polar PIN targeting and transcytosis in plants. *Molecular Plant* **1**: 1056–1066.

Klepikova AV, Kasianov AS, Gerasimov ES, Logacheva MD, Penin AA. **2016**. A high resolution map of the *Arabidopsis thaliana* developmental transcriptome based on RNA-seq profiling. *The Plant Journal* **88**: 1058–1070.

Krejčí J, Stixová L, Pagáčová E, Legartová S, Kozubek S, Lochmanová G, Zdráhal Z, Sehnalová P, Dabravolski S, Hejátko J, *et al.* 2015. Post-translational modifications of histones in human sperm: epigenetics of human sperm. *Journal of Cellular Biochemistry* **116**: 2195–2209.

Kriechbaumer V, Wang P, Hawes C, Abell BM. **2012**. Alternative splicing of the auxin biosynthesis gene *YUCCA4* determines its subcellular compartmentation. *The Plant Journal* **70**: 292–302.

Kumar S, Stecher G, Li M, Knyaz C, Tamura K. **2018**. MEGA X: molecular evolutionary genetics analysis across computing platforms (FU Battistuzzi, Ed.). *Molecular Biology and Evolution* **35**: 1547–1549.

Laňková M, Humpolíčková J, Vosolsobě S, Cit Z, Lacek J, Čovan M, Čovanová M, Hof M, Petrášek J. **2016**. Determination of dynamics of plant plasma membrane proteins with fluorescence recovery and raster image correlation spectroscopy. *Microscopy and Microanalysis* **22**: 290–299.

Lee JH, Ryu H-S, Chung KS, Posé D, Kim S, Schmid M, Ahn JH. **2013**. Regulation of temperature-responsive flowering by MADS-box transcription factor repressors. *Science (New York, N.Y.)* **342**: 628–632.

Leitner J, Petrášek J, Tomanov K, Retzer K, Pařezová M, Korbei B, Bachmair A, Zažímalová E, Luschnig C. **2012**. Lysine63-linked ubiquitylation of PIN2 auxin carrier protein governs hormonally controlled adaptation of *Arabidopsis* root growth. *Proceedings of the National Academy of Sciences* **109**: 8322–8327.

Li H, Wangenheim D, Zhang X, Tan S, Darwish-Miranda N, Naramoto S, Wabnik K, De Rycke R, Kaufmann WA, Gütl D, *et al.* 2021. Cellular requirements for PIN polar cargo clustering in *Arabidopsis thaliana*. *New Phytologist* **229**: 351–369.

Li H-T, Yi T-S, Gao L-M, Ma P-F, Zhang T, Yang J-B, Gitzendanner MA, Fritsch PW, Cai J, Luo Y, *et al.* 2019. Origin of angiosperms and the puzzle of the Jurassic gap. *Nature Plants* **5**: 461–470.

Liao C-Y, Smet W, Brunoud G, Yoshida S, Vernoux T, Weijers D. **2015**. Reporters for sensitive and quantitative measurement of auxin response. *Nature Methods* **12**: 207.

Marquez Y, Brown JWS, Simpson C, Barta A, Kalyna M. **2012**. Transcriptome survey reveals increased complexity of the alternative splicing landscape in *Arabidopsis*. *Genome Research* **22**: 1184–1195.

Marquez Y, Höpfler M, Ayatollahi Z, Barta A, Kalyna M. **2015**. Unmasking alternative splicing inside protein-coding exons defines exitrons and their role in proteome plasticity. *Genome Research* **25**: 995–1007.

Martín G, Márquez Y, Mantica F, Duque P, Irimia M. **2021**. Alternative splicing landscapes in *Arabidopsis thaliana* across tissues and stress conditions highlight major functional differences with animals. *Genome Biology* **22**: 1–26.

Martinière A, Lavagi I, Nageswaran G, Rolfe DJ, Maneta-Peyret L, Luu D-T, Botchway SW, Webb SED, Mongrand S, Maurel C, *et al.* 2012. Cell wall constrains lateral diffusion of plant plasma-membrane proteins. *Proceedings of the National Academy of Sciences* **109**: 12805–12810.

Men S, Boutté Y, Ikeda Y, Li X, Palme K, Stierhof Y-D, Hartmann M-A, Moritz T, Grebe M. **2008**. Sterol-dependent endocytosis mediates post-cytokinetic acquisition of PIN2 auxin efflux carrier polarity. *Nature Cell Biology* **10**: 237–244.

Müller K, Hošek P, Laňková M, Vosolsobě S, Malínská K, Čarná M, Fílová M, Dobrev PI, Helusová M, Hoyerová K, *et al.* 2019. Transcription of specific auxin efflux and influx carriers drives auxin homeostasis in tobacco cells. *The Plant Journal* **100**: 627–640.

Nakabayashi K, Bartsch M, Ding J, Soppe WJJ. **2015**. Seed dormancy in *Arabidopsis* requires self-binding ability of DOG1 protein and the presence of multiple isoforms generated by alternative splicing. *PLoS Genetics* **11**: e1005737.

Nodzyński T, Vanneste S, Zwiewka M, Pernisová M, Hejátko J, Friml J. **2016**. Enquiry into the topology of plasma membrane-localized PIN auxin transport components. *Molecular Plant* **9**: 1504–1519.

Ogura T, Goeschl C, Filiault D, Mirea M, Slovak R, Wolhrab B, Satbhai SB, Busch W. **2019**. Root system depth in Arabidopsis is shaped by *EXOCYST70A3* via the dynamic modulation of auxin transport. *Cell* **178**: 400-412.e16.

O'Leary NA, Wright MW, Brister JR, Ciufo S, Haddad D, McVeigh R, Rajput B, Robbertse B, Smith-White B, Ako-Adjei D, *et al.* 2016. Reference sequence (RefSeq) database at NCBI: current status, taxonomic expansion, and functional annotation. *Nucleic Acids Research* **44**: D733-745.

Pernisova M, Prat T, Grones P, Harustiakova D, Matonohova M, Spichal L, Nodzynski T, Friml J, Hejatko J. **2016**. Cytokinins influence root gravitropism via differential regulation of auxin transporter expression and localization in *Arabidopsis*. *New Phytologist* **212**: 497–509.

Petrasek J, Mravec J, Bouchard R, Blakeslee JJ, Abas M, Seifertová D, Wisniewska J, Tadele Z, Kubes M, Covanová M, *et al.* 2006. PIN proteins perform a rate-limiting function in cellular auxin efflux. *Science (New York, N.Y.)* **312**: 914–918.

Posé D, Verhage L, Ott F, Yant L, Mathieu J, Angenent GC, Immink RGH, Schmid M. **2013**. Temperature-dependent regulation of flowering by antagonistic *FLM* variants. *Nature* **503**: 414–417.

Rademacher EH, Offringa R. **2012**. Evolutionary Adaptations of Plant AGC Kinases: From Light Signaling to Cell Polarity Regulation. *Frontiers in Plant Science* **3**: 250.

Rakusová H, Abbas M, Han H, Song S, Robert HS, Friml J. **2016**. Termination of shoot gravitropic responses by auxin feedback on PIN3 polarity. *Current Biology* **26**: 3026–3032.

Rakusová H, Gallego-Bartolomé J, Vanstraelen M, Robert HS, Alabadí D, Blázquez MA, Benková E, Friml J. **2011**. Polarization of PIN3-dependent auxin transport for hypocotyl gravitropic response in *Arabidopsis thaliana*. *The Plant Journal* **67**: 817–826.

Reddy ASN, Marquez Y, Kalyna M, Barta A. **2013**. Complexity of the alternative splicing landscape in plants. *The Plant Cell* **25**: 3657–3683.

Remy E, Cabrito TR, Baster P, Batista RA, Teixeira MC, Friml J, Sá-Correia I, Duque P. **2013**. A major facilitator superfamily transporter plays a dual role in polar auxin transport and drought stress tolerance in *Arabidopsis*. *The Plant Cell* **25**: 901–926.

Retzer K, Butt H, Korbei B, Luschnig C. **2014**. The far side of auxin signaling: fundamental cellular activities and their contribution to a defined growth response in plants. *Protoplasma* **251**: 731–746.

Robert HS, Grones P, Stepanova AN, Robles LM, Lokerse AS, Alonso JM, Weijers D, Friml J. **2013**. Local auxin sources orient the apical-basal axis in *Arabidopsis* embryos. *Current Biology* **23**: 2506–2512.

Rosquete MR, von Wangenheim D, Marhavý P, Barbez E, Stelzer EHK, Benková E, Maizel A, Kleine-Vehn J. **2013**. An auxin transport mechanism restricts positive orthogravitropism in lateral roots. *Current Biology* **23**: 817–822.

Rosquete MR, Waidmann S, Kleine-Vehn J. **2018**. PIN7 auxin carrier has a preferential role in terminating radial root expansion in *Arabidopsis thaliana*. *International Journal of Molecular Sciences* **19**: 1238.

Roychoudhry S, Kieffer M, Del Bianco M, Liao C-Y, Weijers D, Kepinski S. **2017**. The developmental and environmental regulation of gravitropic setpoint angle in *Arabidopsis* and bean. *Scientific Reports* **7**: 42664.

Rueden CT, Schindelin J, Hiner MC, DeZonia BE, Walter AE, Arena ET, Eliceiri KW. **2017**. ImageJ2: ImageJ for the next generation of scientific image data. *BMC Bioinformatics* **18**: 529.

Ruzicka K, Zhang M, Campilho A, Bodi Z, Kashif M, Saleh M, Eeckhout D, El-Showk S, Li H, Zhong S, *et al.* 2017. Identification of factors required for m6A mRNA methylation in *Arabidopsis* reveals a role for the conserved E3 ubiquitin ligase HAKAI. *New Phytologist* **215**: 157–172.

Shang X, Cao Y, Ma L. **2017**. Alternative splicing in plant genes: a means of regulating the environmental fitness of plants. *International Journal of Molecular Sciences* **18**: 432.

Sibout R, Sukumar P, Hettiarachchi C, Holm M, Muday GK, Hardtke CS. **2006**. Opposite Root Growth Phenotypes of *hy5* versus *hy5 hyh* mutants correlate with increased constitutive auxin signaling. *PLoS Genetics* **2**: e202.

Sievers F, Wilm A, Dineen D, Gibson TJ, Karplus K, Li W, Lopez R, McWilliam H, Remmert M, Söding J, *et al.* 2011. Fast, scalable generation of high-quality protein multiple sequence alignments using Clustal Omega. *Molecular Systems Biology* **7**

Simaskova M, O'Brien JA, Khan M, Van Noorden G, Ötvös K, Vieten A, De Clercq I, Van Haperen JMA, Cuesta C, Hoyerová K, *et al.* 2015. Cytokinin response factors regulate PIN-FORMED auxin transporters. *Nature Communications* **6**: 8717.

Sprague BL, McNally JG. **2005**. FRAP analysis of binding: proper and fitting. *Trends in Cell Biology* **15**: 84–91.

Staiger D, Brown JWS. **2013**. Alternative splicing at the intersection of biological timing, development, and stress responses. *The Plant Cell* **25**: 3640–3656.

Stamm S, Ben-Ari S, Rafalska I, Tang Y, Zhang Z, Toiber D, Thanaraj TA, Soreq H. **2005**. Function of alternative splicing. *Gene* **344**: 1–20.

Swarup K, Benková E, Swarup R, Casimiro I, Péret B, Yang Y, Parry G, Nielsen E, De Smet I, Vanneste S, *et al.* 2008. The auxin influx carrier LAX3 promotes lateral root emergence. *Nature Cell Biology* **10**: 946–954.

Szakonyi D, Duque P. **2018**. Alternative splicing as a regulator of early plant development. *Frontiers in Plant Science* **9**: 1174.

Teale WD, Pasternak T, Dal Bosco C, Dovzhenko A, Kratzat K, Bildl W, Schwörer M, Falk T, Ruperti B, V Schaefer J, *et al.* 2020. Flavonol-mediated stabilization of PIN efflux complexes regulates polar auxin transport. *The EMBO Journal* **40**: e104416.

Tress ML, Abascal F, Valencia A. **2017**. Alternative splicing may not be the key to proteome complexity. *Trends in Biochemical Sciences* **42**: 98–110.

Tseng Q, Duchemin-Pelletier E, Deshiere A, Balland M, Guillou H, Filhol O, Théry M. **2012**. Spatial organization of the extracellular matrix regulates cell-cell junction positioning. *Proceedings of the National Academy of Sciences of the United States of America* **109**: 1506–1511.

Tsugeki R, Tanaka-Sato N, Maruyama N, Terada S, Kojima M, Sakakibara H, Okada K. **2015**. CLUMSY VEIN, the *Arabidopsis* DEAH-box Prp16 ortholog, is required for auxin-mediated development. *The Plant Journal* **81**: 183–197.

Waidmann S, De-Araujo L, Kleine-Vehn J, Korbei B. **2018**. Immunoprecipitation of Membrane proteins from *Arabidopsis thaliana* root tissue. In: Ristova D, Barbez E, eds. Methods in Molecular Biology. Root Development. New York, NY: Springer New York, 209–220.

Waldie T, Leyser O. **2018**. Cytokinin targets auxin transport to promote shoot branching. *Plant Physiology* **177**: 803–818.

Weller B, Zourelidou M, Frank L, Barbosa ICR, Fastner A, Richter S, Jürgens G, Hammes UZ, Schwechheimer C. **2017**. Dynamic PIN-FORMED auxin efflux carrier phosphorylation at the plasma membrane controls auxin efflux-dependent growth. *Proceedings of the National Academy of Sciences* **114**: E887–E896.

Willige BC, Ahlers S, Zourelidou M, Barbosa ICR, Demarsy E, Trevisan M, Davis PA, Roelfsema MRG, Hangarter R, Fankhauser C, *et al.* 2013. D6PK AGCVIII kinases are required for auxin transport and phototropic hypocotyl bending in *Arabidopsis*. *The Plant Cell* **25**: 1674–1688.

Zadnikova P, Petrášek J, Marhavý P, Raz V, Vandenbussche F, Ding Z, Schwarzerová K, Morita MT, Tasaka M, Hejátko J, *et al.* 2010. Role of PIN-mediated auxin efflux in apical hook development of *Arabidopsis thaliana*. *Development* **137**: 607–617.

Zadnikova P, Wabnik K, Abuzeineh A, Gallemi M, Straeten DVD, Smith RS, Inzé D, Friml J, Prusinkiewicz P, Benková E. **2016**. A model of differential growth-guided apical hook formation in plants. *The Plant Cell* **28**: 2464–2477.

Zourelidou M, Absmanner B, Weller B, Barbosa IC, Willige BC, Fastner A, Streit V, Port SA, Colcombet J, Bentem S de la F van, *et al.* 2014. Auxin efflux by PIN-FORMED proteins is activated by two different protein kinases, D6 PROTEIN KINASE and PINOID. *eLife* **3**: e02860.

Zwiewka M, Bilanovičová V, Seifu YW, Nodzyński T. **2019**. The nuts and bolts of PIN auxin efflux carriers. *Frontiers in Plant Science* **10**: 985.

FIGURE TITLES AND LEGENDS

Fig. 1 Alternative splicing (AS) of the *Arabidopsis thaliana PIN7* and *PIN4* genes leads to two evolutionary conserved functionally different transcripts.

(a) Scheme of coding regions of the *PIN3* clade genes in *Arabidopsis thaliana*. The alternative donor splice site at the end of the first exon of *PIN7* and *PIN4*, respectively, but not *PIN3,* results in two transcripts differing in 12 nucleotides. This sequence (orange) corresponds to the protein motif located in the long internal hydrophilic loop of the transporter. There is also an additional *PIN4c* transcript present in publicly available transcriptomes.

(b) Amino acid alignment of the region around the 4-amino acid motif changed by AS in the PIN3 clade proteins (boxed in pink) in *Arabidopsis thaliana*, including the closest PIN paralogs.

(c) Table shows the number of RNA-seq reads spanning the exon1-exon2 junction corresponding to the detected *PIN7* transcripts in selected *Arabidopsis thaliana* tissue sources. Their ratio was calculated as a percentage of total reads mapped to this area, as assessed from the genome browser graphic interface.

(d) Protein sequence alignments showing the conservation of AS in the example PIN7 isoform orthologs among eudicots. For the sequences of PIN7s from *Nicotiana tabacum*, no homologous AS was seen in the corresponding region.

(e) and **(f)** Phototropic bending of the etiolated *pin347* seedlings carrying the *PIN7a-GFP* and *PIN7b-RFP* **(e)**, and the *PIN7a-RFP* and *PIN7b-GFP* constructs **(f)**.

(g) and **(h)** Quantification of the primary root protoxylem defects **(g)** and lateral root primordia initiation **(h)** of the *pin347* seedlings harboring the *PIN7a-RFP* and *PIN7b-GFP* constructs.

In **(e)**, **(f)** and **(h)**, the middle line corresponds to median, the box corresponds to the 25% and 75% quantiles, the whiskers are the minima and maxima, dots represent single data points. The

asterisks indicate a difference between the respective line and the *pin347* mutant (**$P < 0.01$, ***$P < 0.001$ by one-way ANOVA). For each line in each experiment, at least 15 seedlings were analyzed and confirmed on 8 independent transgenic lines.

Fig. 2 The PIN7 AS reporter system shows overlapping PIN7a and PIN7b expression in most tissues of *Arabidopsis*.

(a) A scheme of the *PIN7* splicing reporter, which consists of two separate constructs. The *PIN7a-GFP* part (PIN7A$_1$G) contains two point mutations (dashed arrows) and leads to the frameshift and its subsequent restoration when the *PIN7a* transcript is solely produced. *PIN7b-RFP* reporter (PIN7BR) carries a premature stop codon inside the protruding *PIN7a* region (dashed arrow below).

(b) to **(c)** Overlapping PIN7a-GFP and PIN7b-RFP reporter expression in the root tip **(b)** and in the etiolated hypocotyl following 4 h of unilateral light stimulation **(c)**.

(d) to **(f)** Differential expression of the P7A$_1$G/P7BR reporter in the lateral root primordia **(d)**, in the stomatal lineage ground cells of the cotyledon epidermis **(e)** and in the area covering apical hook **(f)**.

Yellow arrows: direction of unilateral light. White arrows: areas of different reporter expression. For each tissue, at least 9 images were analyzed. Bars, 50 μm on **(b)** to **(e)**, and 100 μm on **(f)**.

Fig. 3 *PIN7a-GFP* and *PIN7b-RFP* cDNAs expressed in the *pin347* knock-out mutant regulate *Arabidopsis* apical hook development and hypocotyl bending in a mutually antagonistic manner.

(a) and **(b)** Subtle phenotypic differences between the wild type and *pin7-2* mutants expressing the *PIN7a-GFP* and *PIN7b-RFP* cDNAs, documented by the temporal analysis of the phototropic bending **(a)**, and apical hook development **(b)**, where even a tendency of mild gain-of-function phenotypes resulting from the PIN7a-GFP expression was detected.

(c) and **(d)** A temporal analysis of etiolated *pin347* seedlings carrying both *PIN7a*-GFP and *PIN7b-RFP* cDNA transgenes during apical hook development **(c)** and hypocotyl phototropic

bending **(d)**. Inset on **(c)**: The levels of the transcript corresponding to *PIN7a-GFP* cDNA in the *pin347* background, normalized to the native *PIN7* levels in the *pin34* lines as determined by qRT-PCR.

The statistical evaluation, summarized below each panel, was conducted on the regions showing approximately linear temporal course ("lin."). lin. 1 (hypocotyl opening plateau phase) on **(a)** and **(d)** and lin. 2 (apical hook maintenance phase) on **(b)** were evaluated as mean angles of each individual by one-way ANOVA. For lin. 2 on **(c)**, and lin. 3 (apical hook opening phase prior to full opening) on **(b)** and **(c)**, the regions were fitted with linear regression, and the y-axis intercepts for each seedling were assessed by one-way ANOVA. For all experiments, at least 15 seedlings were analyzed for each data point. $*P < 0.05$, $**P < 0.01$, $***P < 0.001$ by one-way ANOVA, n. s.: non-significant. Data are means ± S. E.

Fig. 4 Functional analysis of the PIN7a-GFP and PIN7b-RFP interaction.

(a) *PIN7a* but not *PIN7b* cDNA is able to promote the expression of the *DR5v2::GFP* auxin reporter at the internal side of the *Arabidopsis* apical hooks of the *pin347* seedlings. Note the asymmetric distribution of the nuclear-localized signal in the ground tissue and epidermis, instructive for proper apical hook development.

(b) Comparable [^{3}H]-NAA accumulation kinetics in tobacco BY-2 cells following induction of the *G10-90::XVE>>AtPIN7a-GFP* and *AtPIN7b-GFP* transgenes with decreasing doses of β-estradiol.

(c) The effect of 50 μM brefeldin A (BFA) on the intracellular distribution of PIN7a-GFP and PIN7b-RFP in the *Arabidopsis* root tips. Arrows mark the incomplete co-localization of PIN7a and PIN7b in the BFA bodies.

(d) A temporal dynamics of the BFA-mediated aggregation of PIN7a-GFP and PIN7b-GFP inside cells. The values were determined as a ratio of fluorescence intensities between the cytoplasm and PM.

(e) and **(f)** An immunoblot of the anti-RFP-coupled agarose beads precipitates from the protein extracts from the lines expressing *G10-90::XVE>>PIN7a-GFP*, *G10-90::XVE>>PIN7b-GFP* (negative controls) or a cross between *G10-90::XVE>>PIN7a-GFP* and *G10-90::XVE>>PIN7-*

RFP, probed with anti-GFP and anti-RFP antibody, respectively. The electrophoretic gel was loaded with the crude protein extract (input) and immunoprecipitation eluate (eluate) from the *Arabidopsis* seedlings treated with 5 μM β-estradiol **(e)**; the loading control is shown on **(f)**.

(g) and **(h)** PIN7a and PIN7b can form homo- and heteromers on PM *in vivo*. GFP fluorescence lifetime (τ) determined from the tagged PIN7a and PIN7b proteins and compared to the τ of the PIN7a-GFP alone, presented as a representative image heat map **(g)** and quantified on **(h)**. Proteins were expressed under the control of the *G10-90::XVE* promoter in the *Arabidopsis* root tips and induced with 5 μM β-estradiol.

On the box plots, the middle line corresponds to median, the box corresponds to the 25% and 75% quantiles, the whiskers represent the minima and maxima. On **(d)** and **(h)**, the asterisks indicate a difference between the respective protein pair and the PIN7a-GFP control (*$P < 0.05$, ***$P < 0.001$ by one-way ANOVA). On **(d)**, data are means ± S. E. For each line, on **(a)** and **(b)**, n ≥ 9, on **(c)**, **(d)**, **(g)** and **(h)**, n ≥ 12. Bars, 50 μm on **(a)**, 20 μm on **(c)**, and 10 μm on **(g)**.

Fig. 5 cDNA-encoded PIN7a and PIN7b mutually influence their stability within PM, as assessed by fluorescence recovery after photobleaching (FRAP).

(a) Differential FRAP of *PIN7::PIN7a-GFP* and *PIN7::PIN7b-RFP* on PM of cells in the *Arabidopsis* root tips.. The example images of the bleached region (ROI) are shown on the inset.

(b) The FRAP analysis of PIN3Δ-RFP, which lacks the 4 amino acid motif to mimic the properties of the PIN7b isoform (inset), compared to the control *PIN3-GFP* cDNA line in the *Arabidopsis* root tips.

(c) The FRAP of *SCR::PIN7a-GFP* and *SCR::PIN7b-RFP* expressed in the *pin347* mutant background in the *Arabidopsis* root tips. The lines with a single construct are marked as "single", the lines carrying both transgenes are marked as "cross".

(d) The FRAP analysis of BY-2 tobacco cell lines expressing *G10-90::XVE>>AtPIN7a-GFP* and *AtPIN7b-GFP*, following induction with 5 μM β-estradiol.

Data are means ± S. E. For each data point, at least 20 ROIs were measured. The normalized data points were fit with mono-exponential curves. Bar, 5 μm on **(a)**.

SUPPLEMENTAL INFORMATION TITLES AND LEGENDS

Fig. S1 The localization, phenotypic and expression features of the PIN7a and PIN7b splice isoforms.

Fig. S2 Additional *PIN7* cDNA complementation and expression tests.

Fig. S3 Quantitative and qualitative properties of the PIN7a and PIN7b cDNA-based proteins expressed in the BY-2 cells and *Arabidopsis* seedlings.

Fig. S4 Polarity change in response to the gravitropic and phototropic stimuli and additional interaction tests of PIN7 isoforms.

Fig. S5 Additional experiments to the FRAP analysis of the PIN7 isoforms on the plasma membrane.

Table. S1 List of primers used in the study.

Table. S2 Further details to the linear regression analysis used in the morphodynamic experiments (R2).

Table. S3 Further details to the linear regression analysis used in the morphodynamic experiments (average values of the regression line y-axis intercepts and slopes).

Table. S4 Quantification of the RNA-seq reads spanning the exon1-exon2 junction corresponding to the detected PIN4 transcripts in selected *Arabidopsis thaliana* tissue sources.

Methods S1 DNA manipulations and protein work.

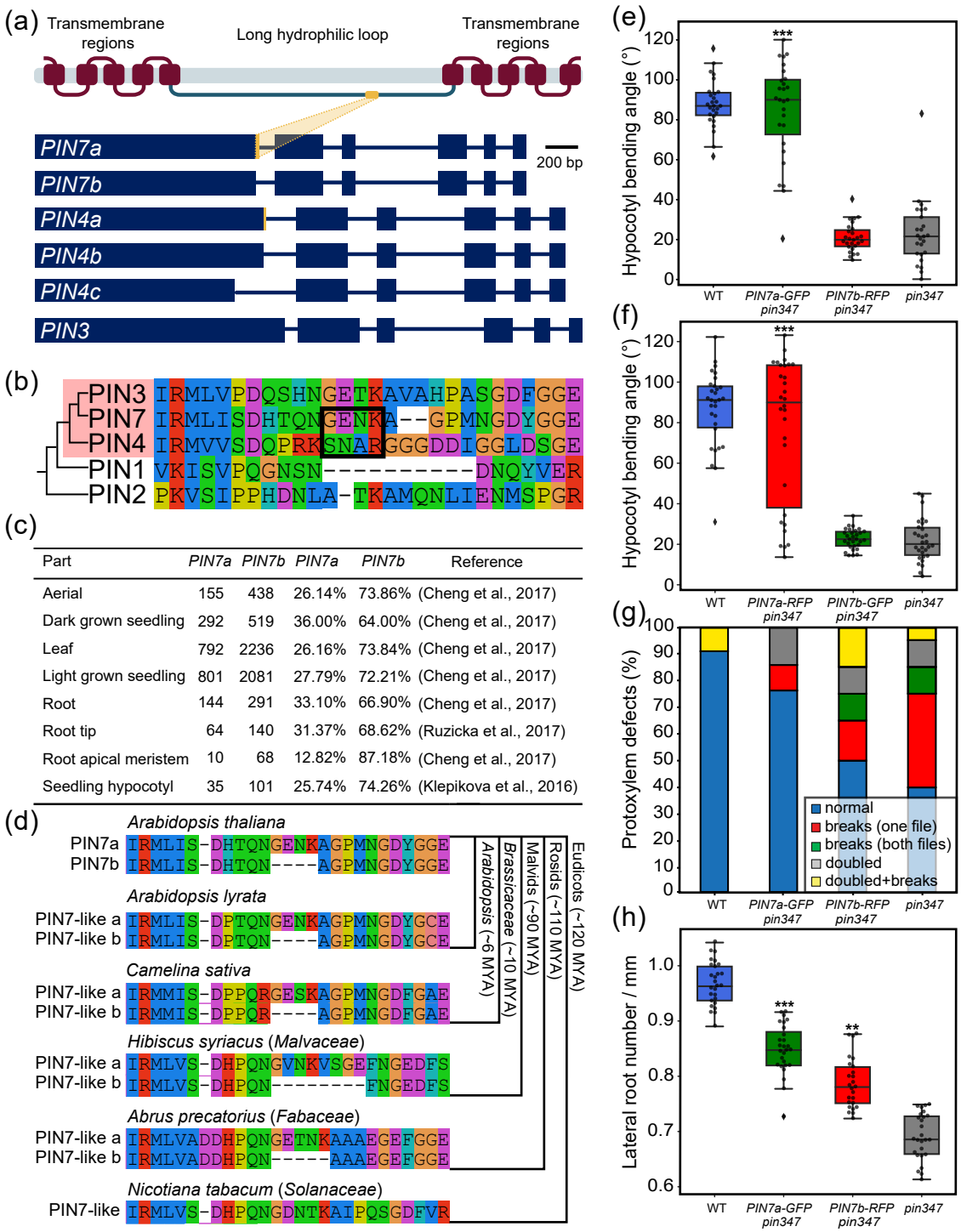

Part	*PIN7a*	*PIN7b*	*PIN7a*	*PIN7b*	Reference
Aerial	155	438	26.14%	73.86%	(Cheng et al., 2017)
Dark grown seedling	292	519	36.00%	64.00%	(Cheng et al., 2017)
Leaf	792	2236	26.16%	73.84%	(Cheng et al., 2017)
Light grown seedling	801	2081	27.79%	72.21%	(Cheng et al., 2017)
Root	144	291	33.10%	66.90%	(Cheng et al., 2017)
Root tip	64	140	31.37%	68.62%	(Ruzicka et al., 2017)
Root apical meristem	10	68	12.82%	87.18%	(Cheng et al., 2017)
Seedling hypocotyl	35	101	25.74%	74.26%	(Klepikova et al., 2016)

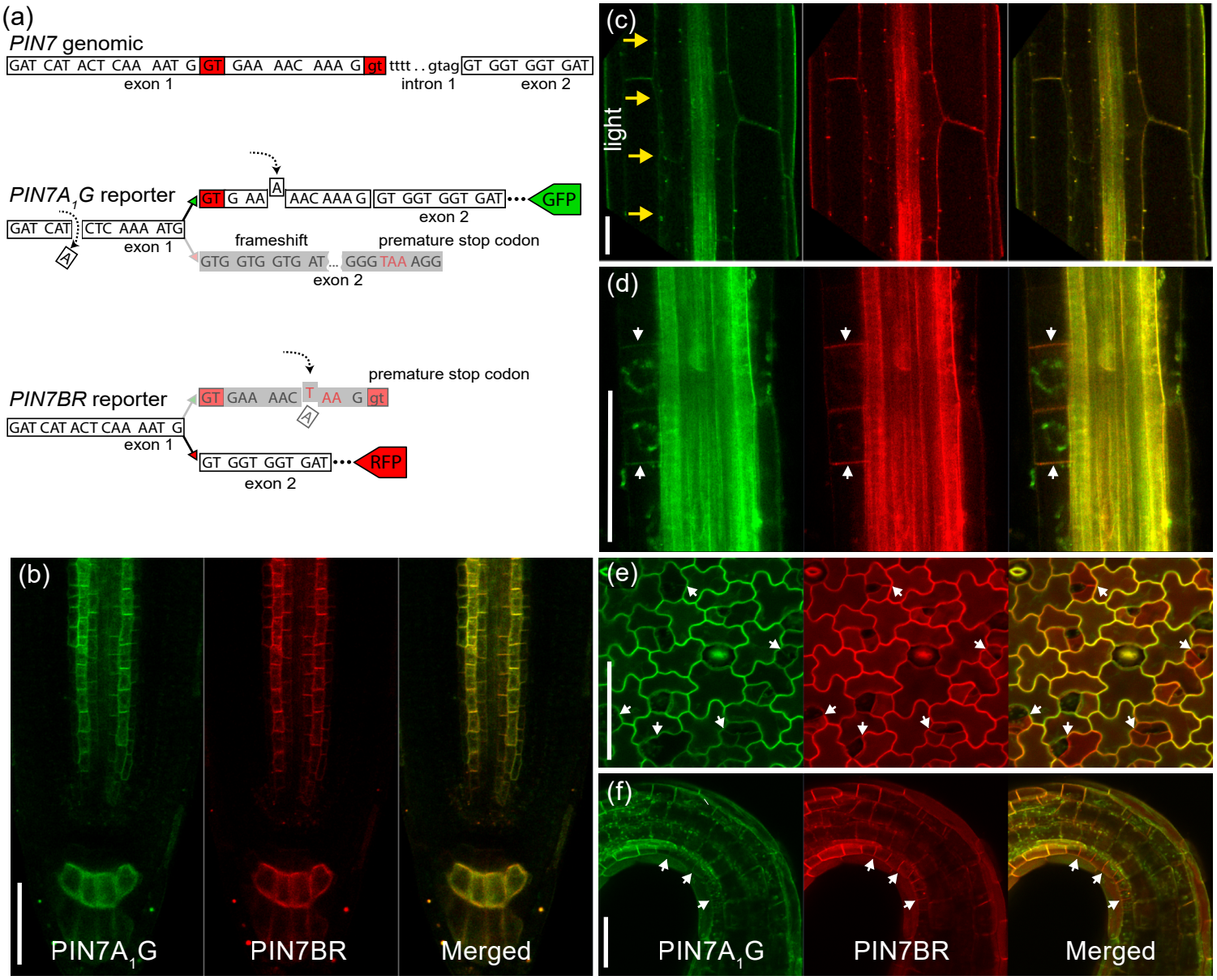
(a)
PIN7 genomic
GAT CAT ACT CAA AAT G GT GAA AAC AAA G gt tttt . . gtag GT GGT GGT GAT
exon 1
intron 1
exon 2
PIN7A1G reporter
GT G AA
A
AAC AAA G
GT GGT GGT GAT
GFP
exon 2
GAT CAT
CTC AAA ATG
exon 1
frameshift
premature stop codon
GTG GTG GTG AT ... GGG TAA AGG
exon 2
premature stop codon
PIN7BR reporter
GT GAA AAC T AA G gt
GAT CAT ACT CAA AAT G
exon 1
GT GGT GGT GAT
RFP
exon 2
(b)
PIN7A1G
PIN7BR
Merged
(c)
light
(d)
(e)
(f)
PIN7A1G
PIN7BR
Merged

(a)

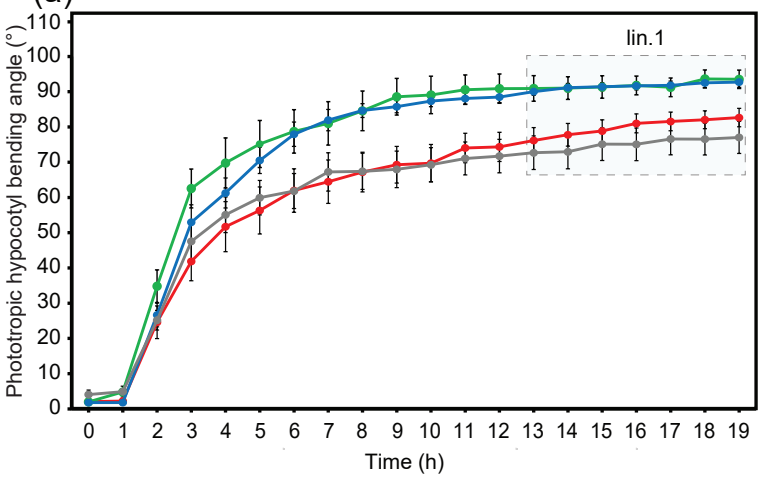

	lin.1
PIN7a-GFP pin7 vs. *pin7*	**
PIN7b-RFP pin7 vs. WT	*

(b)

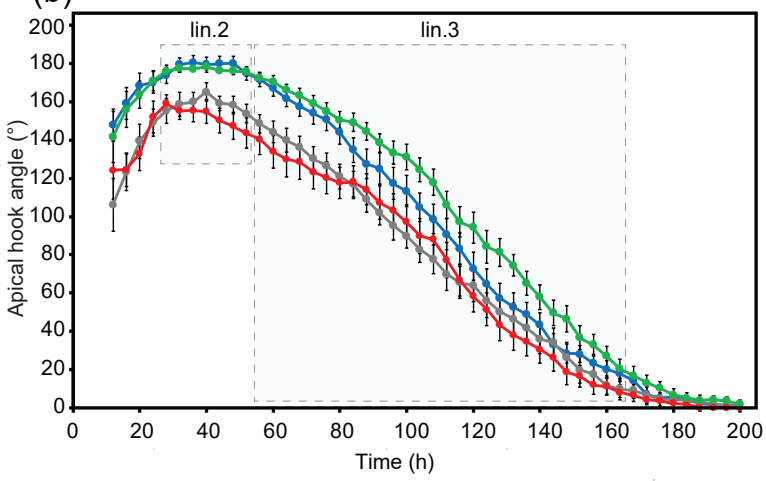

	lin.2	lin.3
PIN7a-GFP pin7 vs. *pin7*	**	*
PIN7b-RFP pin7 vs. WT	***	**

(c)

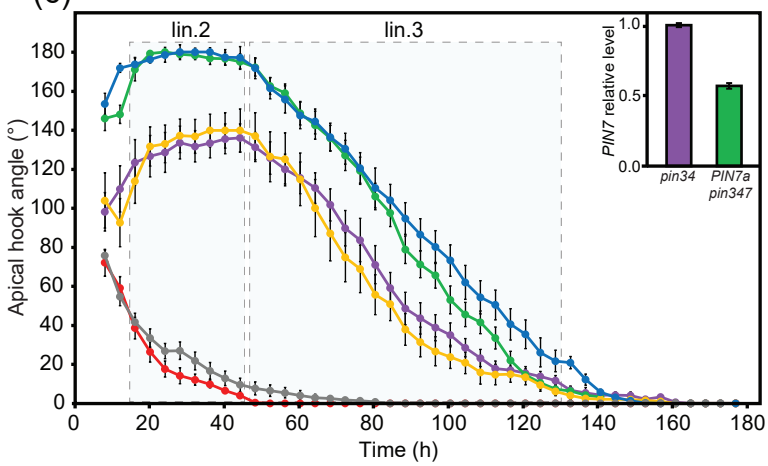

	lin.2	lin.3
PIN7a-GFP pin347 vs. *pin34*	**	***
PIN7a-GFP pin347 vs. WT	n.s.	n.s.
PIN7a-GFP pin347 vs. *PIN7a-GFP* x *PIN7b-RFP pin347*	*	***
PIN7b-RFP pin347 vs. *pin347*	n.s.	n.s.

(d)

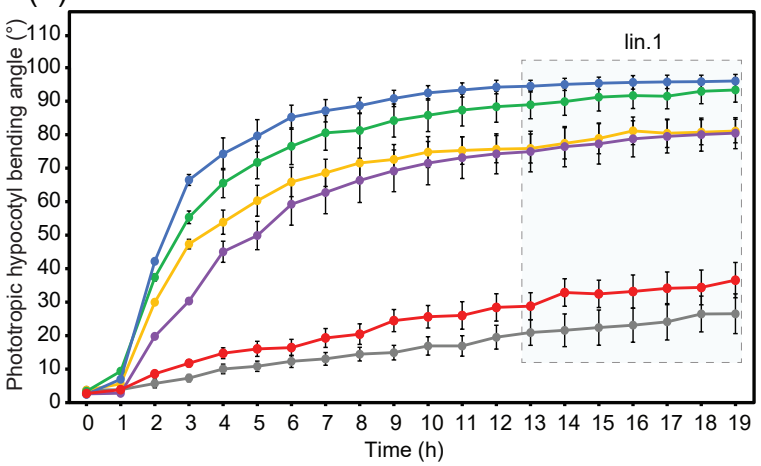

	lin.1
PIN7a-GFP pin347 vs. *pin34*	*
PIN7a-GFP pin347 vs. WT	n.s.
PIN7a-GFP pin347 vs. *PIN7a-GFP* x *PIN7b-RFP pin347*	*
PIN7b-RFP pin347 vs. *pin347*	n.s.

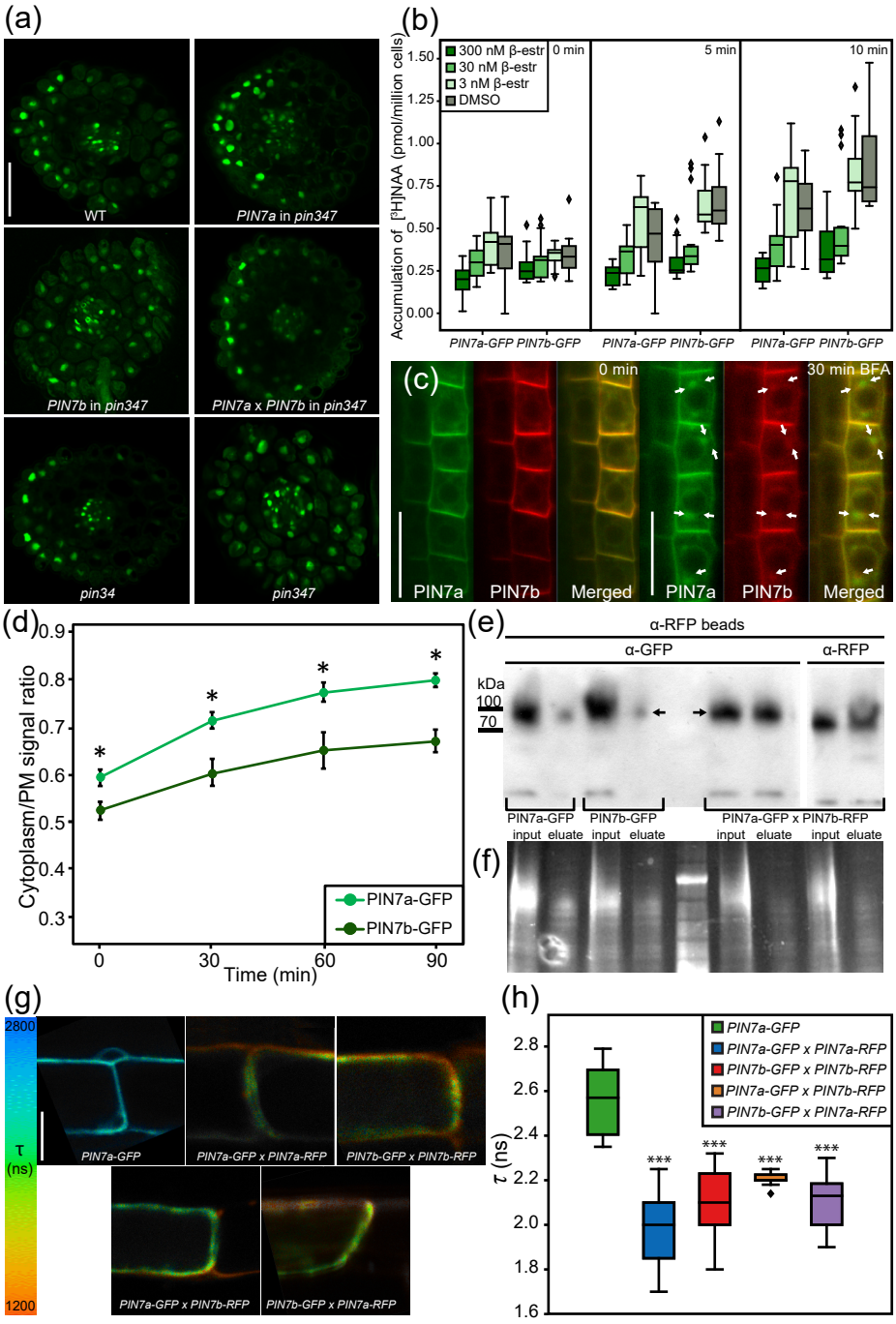
(a)
WT
PIN7a in pin347
PIN7b in pin347
PIN7a x PIN7b in pin347
pin34
pin347
(b)
300 nM β-estr
30 nM β-estr
3 nM β-estr
DMSO
0 min
5 min
10 min
Accumulation of [3H]NAA (pmol/million cells)
PIN7a-GFP PIN7b-GFP
(c)
0 min
30 min BFA
PIN7a
PIN7b
Merged
(d)
Cytoplasm/PM signal ratio
Time (min)
PIN7a-GFP
PIN7b-GFP
(e)
α-RFP beads
α-GFP
α-RFP
kDa
100
70
PIN7a-GFP
PIN7b-GFP
PIN7a-GFP x PIN7b-RFP
input eluate
(f)
(g)
τ (ns)
2800
1200
PIN7a-GFP
PIN7a-GFP x PIN7a-RFP
PIN7b-GFP x PIN7b-RFP
PIN7a-GFP x PIN7b-RFP
PIN7b-GFP x PIN7a-RFP
(h)
τ (ns)
PIN7a-GFP
PIN7a-GFP x PIN7a-RFP
PIN7b-GFP x PIN7b-RFP
PIN7a-GFP x PIN7b-RFP
PIN7b-GFP x PIN7a-RFP

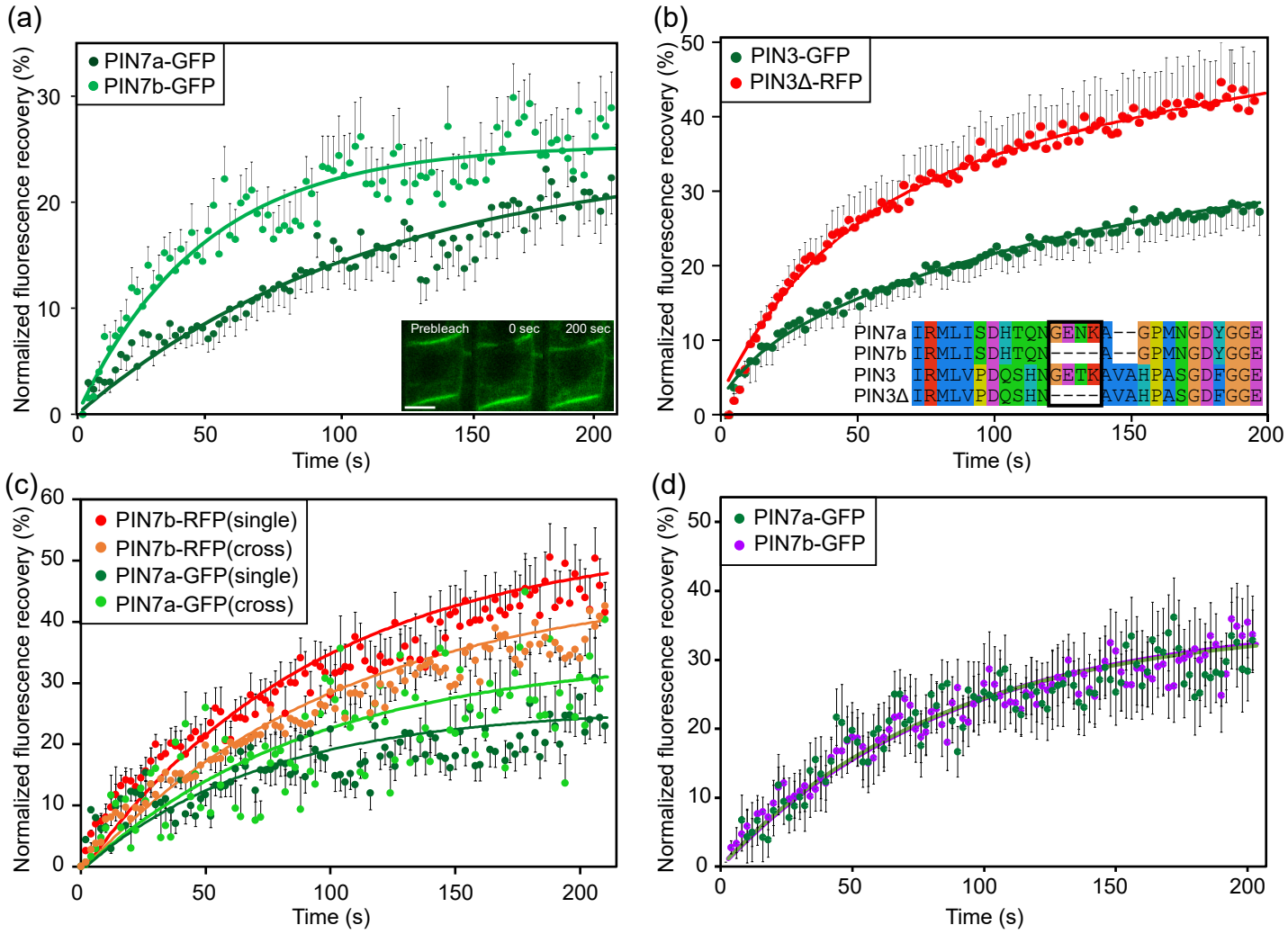
(a)
PIN7a-GFP
PIN7b-GFP
Normalized fluorescence recovery (%)
Time (s)
Prebleach
0 sec
200 sec
(b)
PIN3-GFP
PIN3Δ-RFP
Normalized fluorescence recovery (%)
Time (s)
PIN7a IRMLISDHTQNGENKA---GPMNGDYGGE
PIN7b IRMLISDHTQN-----A---GPMNGDYGGE
PIN3 IRMLVPDQSHNGETKAVAHPASGDFGGE
PIN3Δ IRMLVPDQSHN-----AVAHPASGDFGGE
(c)
PIN7b-RFP(single)
PIN7b-RFP(cross)
PIN7a-GFP(single)
PIN7a-GFP(cross)
Normalized fluorescence recovery (%)
Time (s)
(d)
PIN7a-GFP
PIN7b-GFP
Normalized fluorescence recovery (%)
Time (s)